Check for updates

NIST Special Publication 260
NIST SP 260-260

Certification of Standard Reference Material® 1947a: Great Lakes Fish Tissue

Carolyn Q. Burdette
Kelsey Blevins
Ashley S. P. Boggs
Colleen E. Bryan Sallee
Amy Cuthbertson
Debra Ellisor
N. Alan Heckert
Jennifer C. Hoguet
Kevin Huncik
Amanda Moors
Jennifer Ness
Jessica L. Reiner

This publication is available free of charge from:
https://doi.org/10.6028/NIST.SP.260-260

NIST NATIONAL INSTITUTE OF STANDARDS AND TECHNOLOGY
U.S. DEPARTMENT OF COMMERCE

Page Intentionally Blank

NIST Special Publication 260
NIST SP 260-260

Certification of Standard Reference Material® 1947a: Great Lakes Fish Tissue

Carolyn Q. Burdette, Kelsey Blevins†, Ashley S. P. Boggs, Colleen E. Bryan Sallee, Amy Cuthbertson*, Debra Ellisor, Jennifer C. Hoguet, Kevin Huncik, Amanda Moors, Jennifer Ness, Jessica L. Reiner
Chemical Sciences Division
Materials Measurement Laboratory

N. Alan Heckert
Statistical Engineering Division
Information Technology Laboratory

**Former NIST employee; all work for this publication was done while at NIST*
†Student; all work for this publication was done while at NIST

This publication is available free of charge from:
https://doi.org/10.6028/NIST.SP.260-260

November 2025

U.S. Department of Commerce
Howard Lutnick, Secretary

National Institute of Standards and Technology
Craig Burkhardt, Acting Under Secretary of Commerce for Standards and Technology and Acting NIST Director

NIST SP 260-260
November 2025

Certain equipment, instruments, software, or materials, commercial or non-commercial, are identified in this paper in order to specify the experimental procedure adequately. Such identification does not imply recommendation or endorsement of any product or service by NIST, nor does it imply that the materials or equipment identified are necessarily the best available for the purpose.

NIST Technical Series Policies
Copyright, Use, and Licensing Statements
NIST Technical Series Publication Identifier Syntax

Publication History
Approved by the NIST Editorial Review Board on 2025-11-24

How to Cite this NIST Technical Series Publication
Burdette CQ, Blevins K, Boggs ASP, Bryan Sallee CE, Cuthbertson A, Ellisor D, Heckert NA, Hoguet JC, Huncik K, Moors A, Ness J, Reiner JL (2025) Certification of Standard Reference Material® 1947a: Great Lakes Fish Tissue. (National Institute of Standards and Technology, Gaithersburg, MD), NIST Special Publication (NIST SP) 260-260. https://doi.org/10.6028/NIST.SP.260-260.

Author ORCID iDs

Blevins K:	0000-0002-2939-8097
Boggs ASP:	0000-0001-9765-7559
Bryan Sallee CE:	0000-0002-2334-3925
Burdette CQ:	0000-0002-0843-9224
Cuthbertson A:	0000-0002-7634-3734
Ellisor D:	0000-0002-5980-1887
Heckert NA:	0000-0002-8430-6757
Hoguet JC:	0009-0001-9584-9166
Huncik K:	0009-0004-8039-5563
Moors A:	0000-0002-0864-8464
Ness J:	0000-0002-0035-4373
Reiner JL:	0000-0002-1419-6062

Contact Information
Please address technical questions you may have about this SRM to srms@nist.gov where they will be assigned to the appropriate Technical Project Leader responsible for support of this material. For sales and customer service inquiries, please contact srminfo@nist.gov.

Abstract

Standard Reference Material (SRM) 1947a Great Lakes Fish Tissue is intended to be used in the evaluation of analytical methods for the determination of contaminants, including mercury, polychlorinated biphenyls (PCBs), chlorinated pesticides, polybrominated diphenyl ethers (PBDEs), and per- and polyfluoroalkyl substances (PFAS). The development of SRM 1947a was to create a replacement material for both SRM 1946 Lake Superior Fish Tissue and SRM 1947 Lake Michigan Fish Tissue. This publication documents the production, analytical methods, and statistics used to characterize the material.

Keywords

Fish Tissue; Persistent Organic Pollutants (POPs); Chlorinated Pesticides; Polychlorinated Biphenyls (PCBs), Polybrominated Diphenyl Ethers (PBDEs); Polyfluoroalkyl Substances (PFAS); Reference Material; Mercury

Table of Contents

List of Tables

List of Figures

Acknowledgments

The authors acknowledge Brian Lantry, Annie Schultz, Shonnie Fearon, Theresa Bower, Scott Minihkeim, Terry Lewchanin, Theodore Strang, and Thomas Sanfilippo of the United States Geological Survey (USGS) for the collection and initial preparation of the lake trout tissue used in SRM 1947a Great Lakes Fish Tissue. The authors also acknowledge NIST colleagues John Kucklick, Rebecca Pugh, and Clay Davis for their assistance with the final preparation and analysis of the material, and David Duewer for his substantial contributions to the preparation of this document.

1. Introduction

Natural-matrix fresh-frozen certified reference materials (CRMs) of marine origin such as fish tissue, mussel tissue, and whale blubber have been available from the National Institute of Standards and Technology (NIST) for the determination of a variety of organic contaminants, inorganic content, and organometallic species for over 30 years. These matrices are similar to those often encountered in the analysis of fresh water and marine samples and can be used to validate the complete analytical procedure including extraction, isolation, and quantification of the analytes.

SRMs 1946 Lake Superior Fish Tissue [1] and 1947 Lake Michigan Fish Tissue [2], first released in 2003 and 2007, respectively, were intended primarily for the evaluation of analytical methods for the determination of polychlorinated biphenyl (PCB) congeners, chlorinated pesticides, polybrominated diphenyl ether (PBDE) congeners, perfluorooctane sulfonic acid (PFOS), perfluoroalkyl acids (PFAAs), fatty acids (including omega-3 fatty acids), extractable fat, trace elements, methylmercury, total mercury, proximates, α-hexabromocyclododecane (α-HBCD), and caloric content in fish tissue and similar matrices. All the constituents for which certified or non-certified mass fraction values were provided are naturally present in the fish tissue homogenate. Both materials were prepared from fish caught in 1997.

The sales histories of SRMs 1946 and 1947 over time are displayed in Fig. 1. With the consistent sales of these materials, SRM 1947 sold out in 2022 and SRM 1946 sold out in 2023. As shown in Fig. 2, most sales were to customers within the Unites States of America and Canada.

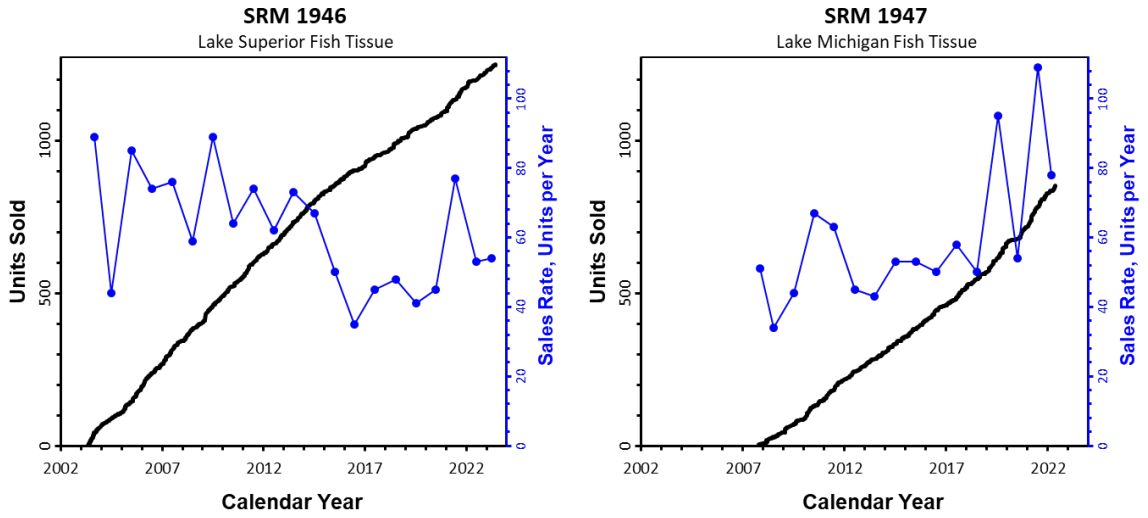

Fig. 1: Sales History of SRMs 1946 and 1947.

The panel to the left displays the sales history of SRM 1946 as a function of time; the panel to the right displays the sales history of SRM 1947. The thick black lines depict the cumulative distribution of sales as functions of the order date; they are plotted using the "Units Sold" axis at the left of each panel. The thin blue lines depict the units sold per year; they are plotted using the "Sales Rate, Units per Year" axis to the right of each panel.

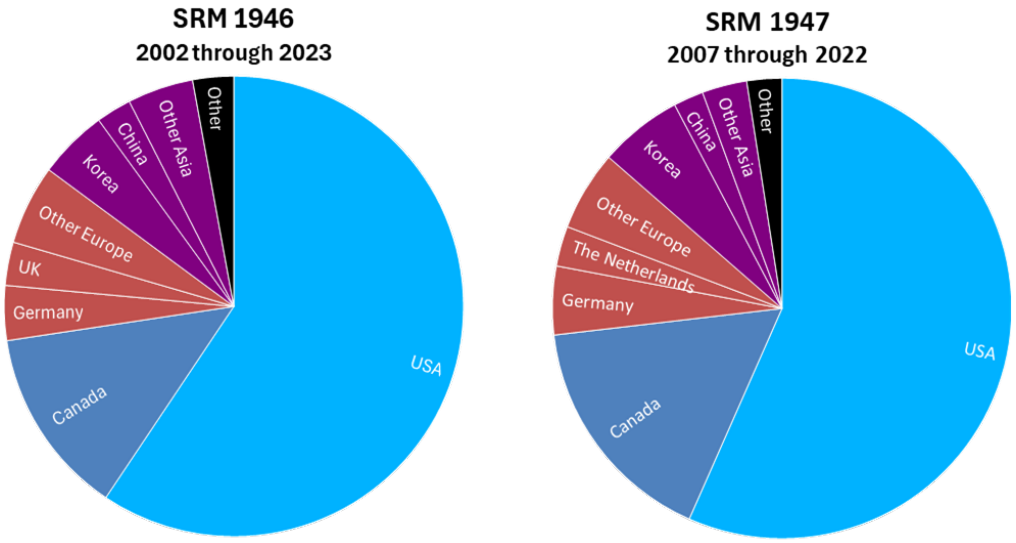

Fig. 2: Location of Customers for SRMs 1946 and 1947.

The panel to the left displays the fraction of SRM 1946 sales to various countries or geographic regions; the panel to the right displays the fraction of SRM 1947 sales. Slices are shown for individual countries only when they purchased at least 3 % of the units sold.

SRM 1947a Great Lakes Fish Tissue, prepared from lake trout captured in Lake Ontario, is designed as a replacement material for both SRM 1946 and 1947. A unit of SRM 1947a consists of four jars each containing approximately 10 g of cryogenically homogenized frozen fish tissue.

2. Production

2.1. Material Collection and Processing

The lake trout utilized for the production of this material were collected by the United States Geological Survey (USGS) from Lake Ontario near Oswego, NY in September 2021. The fish were filleted shortly after being caught, placed in fluorinated ethylene propylene (FEP) bags, and temporarily stored at -20 °C. The filets were shipped overnight on dry ice to NIST (Charleston, SC) and stored at -80 °C in upright freezers. Each bag of filets was partially thawed, chopped into small pieces using titanium knives and refrozen in a liquid nitrogen (LN_2) vapor-phase freezer (≤ -150 °C) until cryomilling. These processing activities resulted in 60.01 kg of material for the production of SRM 1947a.

All bulk material was cryomilled twice using a Palla VM-KT Vibrating cryomill according to established protocols [3] to pulverize the material into a fresh frozen powder and promote blending. Particle size analysis was used as a process indicator for the cryohomogenization procedure. The results obtained following the second round of milling, shown in Table 1, comply with specifications in ISO Standard 13320:2020 Particle size analysis – Laser diffraction methods [4].

Table 1. Particle Size Analysis Results.

	10^{th} Percentile		50^{th} Percentile		90^{th} Percentile	
Cryomilling Round	Diameter, µm	% RSD	Diameter, µm	% RSD	Diameter, µm	% RSD
1	18.6 ± 0.5	2.8	116.0 ± 3.0	2.6	534 ± 38	7.1
2	12.6 ± 0.2	1.9	68.9 ± 0.9	1.3	251 ± 4	1.6

The cryomilling process resulted in approximately 58.81 kg of material.

2.2. Blending and Bottling

The resultant homogenate was packaged in prelabeled glass jars in an LN_2 vapor-phase freezer and stored at -80 °C. Full cases of SRM 1947a (approximately 4900 jars) were transported on dry ice to the Office of Reference Materials in Gaithersburg, MD.

2.3. Research Protections Office

The humane care and treatment of vertebrate animals at NIST is guided by and adheres to the ethical principles set forth in the U.S. Government Principles for the Utilization and Care of Vertebrate Animals Used in Testing, Research, and Training. This study (collection, production, and subsequent use of the material) was reviewed and approved by the NIST Research Protections Office (RPO).

3. Total Mercury (Hg)

3.1. Direct Combustion Atomic Absorption Spectrometry

The mercury mass fraction (as total mercury) in SRM 1947a was investigated using direct combustion atomic absorption spectrometry (DC-AAS) [5] with a DMA 80 direct mercury analyzer (Milestone Scientific, Shelton, CT) [6]. The DMA-80 operates by vaporizing mercury, capturing it through amalgamation, releasing it by desorption, and quantifying it with an atomic absorption spectrophotometer using external calibration.

Samples are first dried at 200 °C and then heated to 650 °C, causing organic materials to be decomposed and mercury to be vaporized in a carrier gas of oxygen which is introduced into a quartz catalyst tube. A continuous flow of oxygen carries the decomposition products through a hot catalyst bed where halogens, nitrogen, and sulfur oxides are trapped. All mercury species are reduced to mercury oxide and are then carried along with reaction gases to a gold amalgamator where the mercury is deposited on gold-covered molecular sieves. All non-mercury vapors and decomposition products are carried out of the system with the continuous gas stream. The mercury deposits are then desorbed as the amalgamator is heated. Vaporized mercury is transported to the spectrophotometer for analysis.

The spectrophotometer uses a mercury vapor lamp as its light source. Light from the lamp is directed through an excitation filter before it irradiates the vaporized mercury contained in a cuvette block with a dual-cell arrangement. The detector utilizes two sequential cells positioned along the optical path of the spectrophotometer: one for low concentration samples (cell 1) and the other for high concentration samples (cell 2). Light which is not absorbed by the mercury vapors then passes through an emission filter before being measured by the detector. Absorbance is measured at 253.7 nm as a function of mercury content.

3.1.1. Materials

Six jars of SRM 1947a were analyzed. Two jars of SRM 1946 Lake Superior Fish Tissue were used as the control material. One unit of SRM 3133 Mercury Standard Solution [7] was used to make the calibration curve solutions. Four pre-cleaned nickel weigh boats were used as procedural blank samples.

3.1.2. Measurement Process

The mass fraction of total Hg was determined with by DC-AAS using external calibration.

Calibration solutions were gravimetrically prepared as aqueous dilutions of SRM 3133 using a Sartorius Model MSE524S balance. The cell 1 low-end and cell 2 high-end calibration curves were prepared on the same day by gravimetrically aliquoting different masses between (0.0775 and 0.5045) g of a calibration solution into pre-cleaned quartz sample boats and weighed using a Sartorius Model ED224S balance. The method parameters for calibration were: 90 s ramp to 200 °C, 30 s hold, 90 s ramp to 650 °C, 180 s hold.

Mercury was measured in the SRM 1947a and 1946 samples by weighing approximately 250 mg and 140 mg, respectively, of material into pre-cleaned nickel sample boats. When the jars were removed from the -80 ° C freezer, they were place in a cooler with dry ice to keep them frozen while sampling. Prior to removing a sub-sample from the jar with a disposable polypropylene (PP) spatula, the lid and body of the jar was wiped down with a Texwipe (CleanPro® Cleanroom Products, Minnetonka, MN) to remove frost before the lid was removed for sampling. The fish tissue samples were placed into the instrument auto-sampler rotor and analyzed sequentially. The method parameters for fish tissue were: 90 s ramp to 200 °C, 30 s hold; 90 s ramp to 400 °C, 30 s hold, 90 s ramp to 650 °C, 180 s hold.

Procedural blanks (empty nickel weighing boats) and SRM 1946 control material samples were bracketed between blocks of SRM 1947a samples to verify instrument calibration and monitor instrumental drift.

3.1.3. Calibration

External peak area versus ng Hg calibration functions were constructed from the DC-AAS peak area signal, A_{Hg}, and Hg amount, A_{Hg}, measurement results shown in Fig. 3.

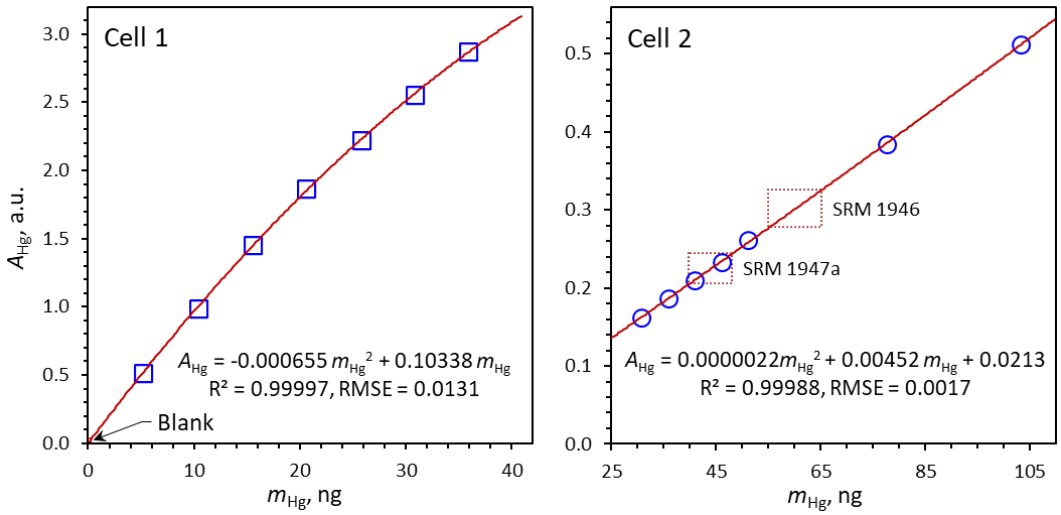

Fig. 3: Calibration Data and Functions for Cell 1 and Cell 2.

Symbols represent {peak area in arbitrary units, Hg amount in ng} results from cell 1 (left panel) and cell 2 (right panel) of the DC-AAS detector. Lines represent the calibration function derived from the calibration data. Calibration model parameters are given in textbox; the root mean square error (RMSE) is the expected difference between an observed and regression model estimated peak area. Dotted-line boxes enclose the sections of the calibration model used to estimate Hg mass fractions.

A second order (quadradic) model was used with both the cell 1 (long path) and cell 2 (short path) data to account for non-ideal Beer-Lambert Law behavior.

$$A_{\mathrm{Hg}} = a \times m_{\mathrm{Hg}}^2 + b \times m_{\mathrm{Hg}} + c\ . \quad (1)$$

where: A_{Hg} is the measured cell 1 mercury peak area,
a, b, and *c* are the parameters of the quadratic model, and
m_{Hg} is the gravimetrically determined amount of Hg.

3.1.4. Procedural Blank Analysis

The constant term, *c*, for the cell 1 data provided by unconstrained quadratic regression is very small compared to its asymptotic standard error, (-0.0022 ± 0.0110) ng. Second order parameter values from regression constrained to go through the origin and measured peak areas were used to estimate the mass fraction of Hg in procedural blanks:

$$w_{\mathrm{Hg},i} = \frac{-b + \sqrt{b^2 + 4\,a\,A_{\mathrm{Hg,i}}}}{2\,a\,m_{\mathrm{blank}}} \quad (2)$$

where: $w_{\mathrm{Hg},i}$ is the apparent mass fraction of mercury in the i^{th} blank,
a and *b* are the parameter values of the constrained cell 1 quadratic model,
$A_{\mathrm{Hg},i}$ is the measured cell 1mercury peak area for the i^{th} blank, and
m_{blank} is the 1 g nominal mass of the empty nickel weigh boats.

The mean blank and its standard uncertainty are calculated from the measurements of the four blanks listed in Table 2.

Table 2. DC-AAS Results for Procedural Blanks.

Blank	m_{blank}, g	A_{Hg}, a.u.	w_{Hg}, ng/g
1	1	0.0102	0.0987
2	1	0.0354	0.3432
3	1	0.0176	0.1704
4	1	0.0359	0.3480
		n [a]:	4
		$\bar{x}$ [b]:	0.240
		s [c]:	0.125
		$u(\bar{x})$ [d]	0.063

a: number of measurements, b: mean, c: standard deviation, d: standard uncertainty of the mean ($s/\sqrt{n}$)

The Hg mass fraction of SRMs 1947a and 1946 samples were blank corrected by subtracting the mean of the procedural blank measurements.

3.1.5. Fish Tissue Analysis

The constant term, *c*, for the cell 2 data provided by unconstrained quadratic regression is not small compared to its asymptotic standard error, (0.0213 ± 0.0056) ng. Second order parameter

values from unconstrained regression and measured peak areas were used to estimate the mass fraction of Hg in the SRM 1947a and 1946 fish tissue samples:

$$w_{\mathrm{Hg},i} = \frac{-b + \sqrt{b^2 + 4\,a\,\left(A_{\mathrm{Hg,i}} - c\right)}}{2\,a\,m_{\mathrm{sample},i}} - m_{\mathrm{blank}} \qquad (3)$$

where: $w_{\mathrm{Hg},i}$ is the wet mass fraction of mercury in the i^{th} sample,
$A_{\mathrm{Hg},i}$ is the measured cell 2 mercury peak area for the i^{th} sample,
a, b and *c* are the parameter values of the unconstrained cell 2 quadradic model,
$m_{\mathrm{sample,i}}$ is the measured mass of the i^{th} sample, and
m_{blank} is the mean of the four procedural blanks.

The estimated total Hg mass fractions for the SRM 1946 and 1947 samples are listed in Table 3. The values are displayed as functions of the jar identifiers in Fig. 4.

Table 3. DC-AAS Results and Summary Statistics for SRM 1946 and SRM 1947a Samples.

SRM 1946				SRM 1947a			
Jar	m_{sample}, g	A_{Hg}, a.u.	w_{Hg}, ng/g	Jar	m_{sample}, g	A_{Hg}, a.u.	w_{Hg}, ng/g
A-1	0.1409	0.3034	430.0	1-A	0.2556	0.2305	177.0
A-2	0.1506	0.3259	433.4	1-B	0.2536	0.2254	174.1
A-3	0.1498	0.3206	428.4	2-A	0.2785	0.2422	171.3
A-4	0.1263	0.2780	437.7	2-B	0.2589	0.2285	173.1
B-1	0.1387	0.3103	447.2	3-A	0.2420	0.2187	176.6
B-2	0.1464	0.3190	436.1	3-B	0.2434	0.2142	171.6
B-3	0.1560	0.3249	417.1	4-A	0.2667	0.2446	180.8
B-4	0.1347	0.2910	430.6	4-B	0.2482	0.2175	171.1
				5-A	0.2664	0.2351	173.4
				5-B	0.2430	0.2059	164.6
				6-A	0.2455	0.2180	173.4
				6-B	0.2576	0.2275	173.1
		n [a]:	8			n [a]:	12
		$\bar{x}$ [b]:	432.6			$\bar{x}$ [b]:	173.3
		s [c]:	8.6			s [c]:	3.9
		$u(\bar{x})$ [d]	3.1			$u(\bar{x})$ [d]	1.1

a: number of measurements, b: mean, c: standard deviation, d: standard uncertainty of the mean ($s/\sqrt{n}$)

The observed total Hg results for SRM 1946 are in excellent agreement with its certified (433 ±9) ng/g 95 % level of confidence interval. This suggests that the SRM 1947a estimated values are unbiased estimates of total Hg.

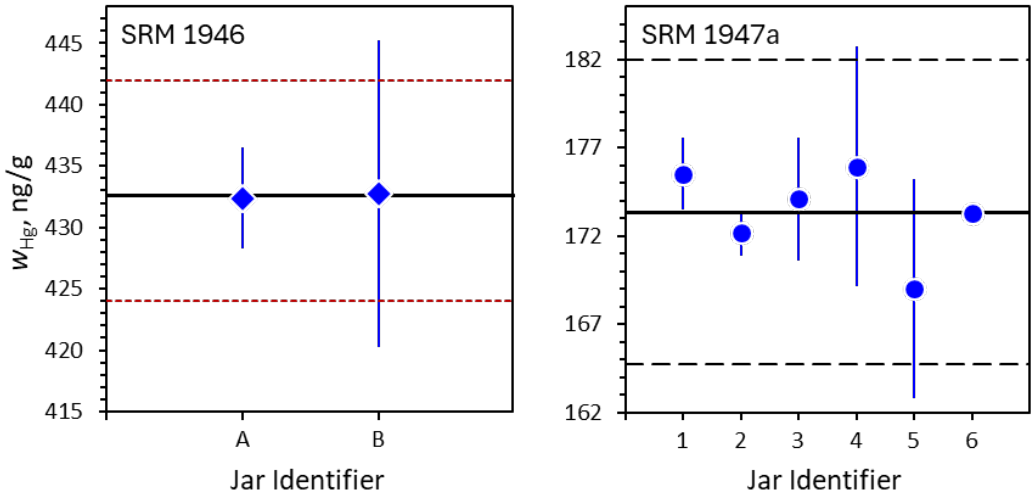

Fig. 4: DC-AAS Results for SRM 1946 and SRM 1947a Samples.

The two diamond symbols (left panel) each represent the mean mass fraction total Hg estimates for four sub-samples from one SRM 1946 jar. The six circle symbols (right panel) each represent the mean mass fraction total Hg estimates for two sub-samples from one SRM 1947a jar. The error bars represent one standard deviation. The thick solid lines represent all-subsample means. The short-dash lines in the left panel bound the certified 95 % level of confidence interval for total Hg in SRM 1946. The long-dash lines in the right panel bound the SRM 1947a (mean ± standard deviation) interval.

3.1.6. Uncertainty Budgets

Table 4 lists the components of uncertainty for total Hg measurements in the SRM 1946 and 1947a fish tissues. Single factor analysis of variance (ANOVA) indicates no statistically significant between-jar variability in either of the SRMs. The measurement result for each subsample is therefore regarded as an independent estimate of total Hg. The sample replication estimates for both SRMs are therefore based on the total number of subsamples analyzed.

Table 4. Uncertainty Components for DC-AAS Estimated Total Hg in SRMs 1946 and 1947a

Source	Symbol	Basis
Sample replication	$u(A_{sample})$	Standard uncertainty of the mean of subsample measurements, with degrees of freedom n - 1
Blank correction	$u(A_{blank})$	Standard uncertainty of the mean of blank measurements
Weighing uncertainty	$u(B_{weigh})$	Standard uncertainty of calibration, drift (temporal and electrostatic) and relative impact on weighing measurements. Estimated at 0.1 % relative
SRM 3133	$u(B_{SRM})$	Standard uncertainty derived from the certified value of SRM 3133, (10.004 ±0.040) mg/g, with the expanded uncertainty divided by a coverage factor k = 2.183
Calibration model	$u(B_{cal})$	Standard uncertainty derived from the root mean square error (RMSE) of the quadratic model

The over-all total Hg standard uncertainty for the fish tissue measurements combine these uncertainty sources in quadrature:

$$u(w_{\mathrm{Hg}}) = \sqrt{u^2(A_{\mathrm{sample}}) + u^2(A_{\mathrm{blank}}) + u^2(B_{\mathrm{weigh}}) + u^2(B_{\mathrm{SRM}}) + u^2(B_{\mathrm{cal}})} \qquad (4)$$

The estimated values for these components and the 95 % level of confidence expanded uncertainties for the SRM 1946 and 1947a DC-AAS measurements are presented in Table 5

Table 5. Uncertainty Budget for DC-AAS Total Hg in SRM 1946 and SRM 1947a.

	SRM 1946		SRM 1947a	
Source	u_i	DF	u_i	DF
Sample replication	3.1	7	1.1	11
Blank correction	0.1	3	0.1	3
Weighing uncertainty	0.4	60	0.2	60
Primary calibrant (SRM 3133) uncertainty	0.8	11.8	0.3	11.8
Calibration curve linear fit uncertainty	2.5	4	1.4	4
Combined standard uncertainty	4.0	12	1.8	10
Student's t 95 % coverage factor	2.18		2.23	
95 % level of confidence expanded uncertainty	8.8		4.1	

3.1.7. Metrological Traceability

The measured total Hg mass fraction is metrologically traceable to the International System of Units (SI) through use of SRM 3133 Mercury Standard Solution (Lot #160921) as the calibrant.

3.2. Isotope Dilution Cold-Vapor Inductively Coupled Plasma Mass Spectrometry

The mercury mass fraction in SRM 1947a was investigated using Isotope Dilution Cold-Vapor Inductively Coupled Plasma Mass Spectrometry (ID-CV-ICP-MS) [8]. The method is based on reduction of Hg(II) in acidic solution with tin (II) chloride, and transfer of the resulting "cold vapor" to an inductively coupled plasma mass spectrometer (ICP-MS) for measurement. The method is extremely sensitive, permitting quantitation down to approximately 10 pg/g, in any matrix. This is possible because the transfer of mercury in the gas phase is highly efficient and selective. The process is illustrated in Fig. 5.

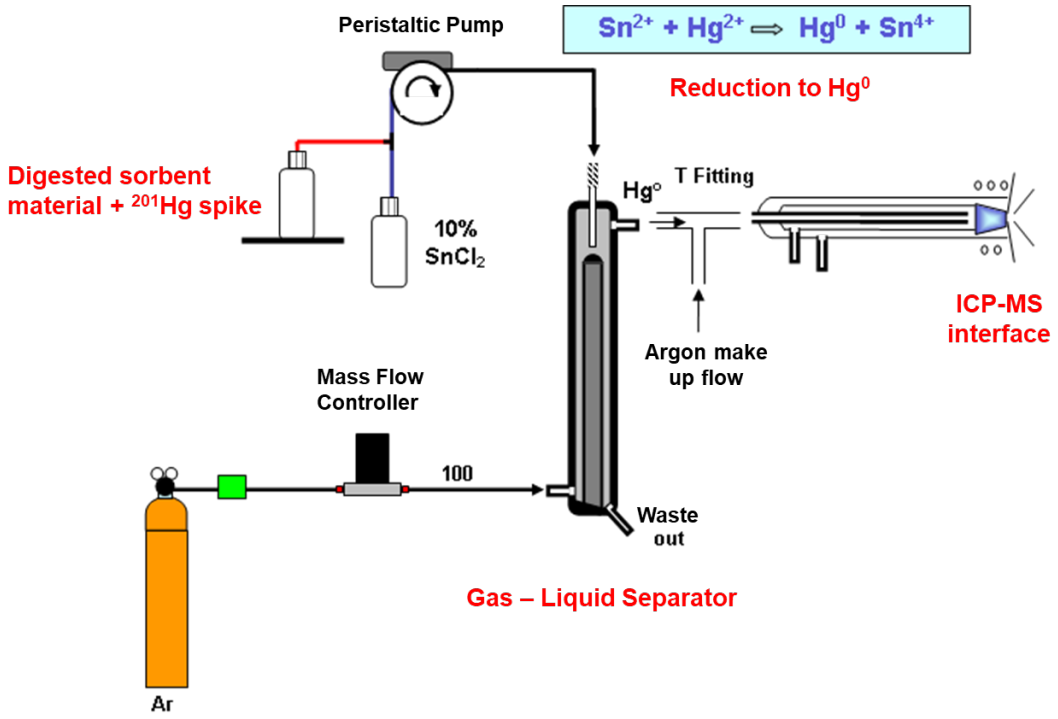

Fig. 5: Configuration for measurements by ID-CV-ICP-MS.

The $^{201}Hg^{2+}$ isotopically spiked sample is dynamically reduced with $SnCl_2$. Hg^0 vapor is separated from the liquid and swept into the ICP-MS for analysis.

Sample aliquots containing mercury are equilibrated with an enriched isotopic spike and the ratio of the spike isotope to a reference isotope is measured by ICP-MS. The measured ratio is used as an input variable for the isotope dilution equation, from which highly accurate data can be obtained for the target analyte. A quadrupole ICP-MS system can be cycled relatively rapidly between isotopes, and therefore the attainable isotope ratio measurement repeatability is of the order of (0.1 to 0.3) %. Because isotope dilution is employed, matrix effects are not a significant factor. However, spectral interferences must be accounted for and eliminated if necessary.

3.2.1. Experimental Design

The study was designed to optimize the analytical system for accurate isotope dilution measurements. The mass fraction of total Hg in SRM 1947a was well known through value assignment of the material by DC-AAS (Section 3.1). The isotope dilution measurement system was designed to optimize sample mass and amount of added ^{201}Hg spike. Four procedural blank measurements were considered sufficient for these determinations. The spike to sample ratio $^{201}Hg/^{202}Hg \approx 2$ provided a compromise between reducing the effects of error magnification, ICP-MS instrument background, and minimizing ICP-MS detector dead-time resulting from a measured isotope ratio differing from unity.

3.2.2. Materials

The same six jars of SRM 1947a analyzed by DC-AAS were analyzed by ID-CV-ICP-MS. Two jars of SRM 1946 Lake Superior Fish Tissue were used as the control material. One unit of SRM 3133 Mercury Standard Solution (Lot No. 160921) was used to make the calibration curve solutions. Hg-201 spike (Batch 180691) was purchased from the National Isotope Development Center (NIDC) (Oak Ridge, TN).

3.2.3. Sample Preparation

When the jars of SRM 1947a and SRM 1946 were removed from the -80 ° C freezer to remove sub-samples for analysis, they were placed in a cooler with ice packs to keep them frozen while sampling. Prior to removing a sub-sample from the jar with a disposable PP spatula, the lid and body of the jar were wiped down with a Texwipe (CleanPro® Cleanroom Products, Minnetonka, MN) to remove frost before the lid was removed for sampling. Single sub-samples from each jar of SRM 1947a and triplicate sub-samples from each jar of SRM 1946, approximate nominal mass 0.5 g, were accurately weighed by difference into quartz vessels using a calibrated four-place analytical balance (Sartorius Model MSE524S) and spiked with an accurately weighed aliquot of ^{201}Hg spike, followed by the addition of 6 g high purity nitric acid (HNO_3) (Optima, Fisher Scientific, Suwanee, GA).

Microwave digestion was carried out in an Anton Paar (Ashland, VA) Multiwave 5000 microwave using the following manufacturer's "Food (Fat-Rich)" method: 600 watts of power, 20 min ramp; 1200 watts of power, 15 min ramp and 15 min hold; 15 min cool down at 0 power. Microwave temperature and pressure limits for this method were set to 280 ℃ and 8 MPa (80 bar), respectively. After cooling to room temperature, the vessel contents were transferred to 50 mL PP centrifuge tubes and initially diluted with high purity deionize water (18.3 Ω) to approximately 25 mL until diluted further on the day of measurement.

Analytical measurements were completed within one day of final dilution to reduce the risk of external contamination and Hg losses from the solutions during storage. On the day of measurement, samples were diluted to approximately 0.3 ng/g ^{201}Hg, which was suitable for measurement by cold-vapor ICP-MS, and approximately 1.0 g (approximately 2 % in final dilution) of high-purity hydrochloric acid (HCl) (Fisher Scientific, Suwanee, GA) was added to each sample for additional Hg stabilization.

In addition to the samples and controls, four procedural blanks, containing a small aliquot of ^{201}Hg spike only, were carried through the entire sample processing and measurement scheme.

3.2.4. Measurement Process

Mercury measurements were made using cold-vapor Hg generation coupled with ICP-MS isotope ratio measurements [8]. The Hg vapor was generated using tin (II) chloride reductant (10 % mass fraction in 7 % volume fraction HCl) and separated from the liquid phase using a commercial glass reaction/separator cell (Teledyne CETAC, Omaha, NE). The vapor was transferred to Thermo Electron X Series II ICP-MS (Thermo Fisher Scientific, Waltham, MA) with

1/16" (1.6 mm) i.d. Viton tubing, using an argon carrier gas flow rate of approximately 100 mL/min. This gas stream was mixed with the plasma injector gas stream using a plastic T piece.

The ICP-MS was operated in a dry plasma mode, which necessitated slight re-tuning of the ion lenses relative to an aqueous aerosol sample introduction system. All samples were transferred to the instrument in manual sequence, and the timing of the sample uptake was adjusted to allow sufficient time to measure the instrument background prior to measurement of the sample. The ^{201}Hg and ^{202}Hg isotopes were monitored for a duration of 60 s in a pulse counting Time-Resolved-Analysis mode (TRA) to recover the individual ion count rates. The isotope-time profiles were downloaded as CSV files to a Microsoft Excel spreadsheet for calculation of background corrected ^{201}Hg/^{202}Hg ratios using Isotope Dilution Assistant (IDA) [9]. The instrument detector dead-time was 37 ns.

3.2.5. Spike Calibration

The working ^{201}Hg isotopic spike solution was prepared by accurate gravimetric dilution of a master stock solution, which was calibrated by reverse isotope dilution using the high-purity primary standard SRM 3133. Stock solutions were prepared by serial dilution. Four spike calibration mixtures (approximately 0.3 ng/g ^{201}Hg) were prepared from these stock solutions (approximately 50 ng/g ^{201}Hg), and these were measured using cold-vapor ICP-MS, under the same conditions as the samples (reverse ID-MS).

3.2.6. Quantitative Measurements

The relationship used to estimate the individual sample ID-CV-ICP-MS mass fractions is:

$$w_{\mathrm{Hg}} = 1000 \left(\frac{m_{201\mathrm{Hg}}\, K}{m_{\mathrm{sample}}} \right) \left(\frac{B_s - A_s\, F\, R}{A\, F\, R - B} \right) \qquad (5)$$

where: w_{Hg} is the wet mass fraction of mercury in the sample (ng/g),
$m_{201\mathrm{Hg}}$ is the mass of ^{201}Hg spike added (µg),
m_{sample} is the mass of sample aliquot taken (g),
K = 0.997847 is the natural to spike (^{202}Hg/^{201}Hg) atomic weight ratio [10,11],
A_s = 2.62 atom % is the fractional abundance of the reference isotope (^{202}Hg) in the spike,
B_s = 96.17 atom % is the fractional abundance of the spike isotope (^{201}Hg) in the spike,
A = 29.74 atom % is the natural fractional abundance of the reference isotope (^{202}Hg) [12],
B = 13.17 atom % is the natural fractional abundance of the spike isotope (^{201}Hg) [12],
F = 1 is the discrimination correction factor for measured ratio R, and
R is the detector dead-time corrected ^{202}Hg/^{201}Hg ratio.

The A_s and B_s values are specific to the NIDC “Hg-201 spike (Batch 180691)” spiking solution.

The ^{202}Hg counts in the four procedural blanks were about the same as the instrument background signal. The sample measurement data were therefore not blank-corrected.

There are no commonly recognized spectral interferences for *m/z* 201 and *m/z* 202. The isotopic composition of Hg has no significant natural variability that is measurable on a quadrupole ICP-MS. Therefore, the isotopic composition of the SRM 1947a and SRM 1946 samples was not expected to deviate from that of the accepted natural composition.

The results of the ID-CV-ICP-MS analyses are listed in Table 6; they are displayed in Fig. 6.

Table 6. ID-CV-ICP-MS Results and Summary Statistics.

Microwave Vessel	Sample ID	m_{sample} g	m_{201Hg} µg	$\frac{^{202}Hg}{^{201}Hg}$	m_{Hg} µg	w_{Hg} ng/g
R1-2	SRM 1946 A-1	0.5097	0.11066	1.9687	0.2215	434.5
R1-3	SRM 1946 A-2	0.5432	0.11052	1.8934	0.2332	429.2
R2-16	SRM 1946 A-3	0.5055	0.11084	1.9773	0.2205	436.2
R1-4	SRM 1946 B-1	0.5171	0.11070	1.9513	0.2242	433.6
R2-14	SRM 1946 B-2	0.5196	0.11048	1.9397	0.2256	434.1
R2-15	SRM 1946 B-3	0.5486	0.11240	1.8842	0.2387	435.1
					n [a]:	6
					$\bar{x}$ [b]:	433.8
					s [c]:	2.4
					$u(\bar{x})$ [d]	1.0
R1-6	SRM 1947a Jar 1	0.5062	0.04321	1.9193	0.0895	176.8
R1-7	SRM 1947a Jar 3	0.5163	0.04301	1.9009	0.0903	174.8
R1-8	SRM 1947a Jar 5	0.5012	0.04295	1.9140	0.0893	178.2
R2-10	SRM 1947a Jar 6	0.5535	0.04536	1.8359	0.0998	180.3
R2-11	SRM 1947a Jar 9	0.5123	0.04291	1.9072	0.0896	175.0
R2-12	SRM 1947a Jar 10	0.5482	0.04520	1.8964	0.0951	173.6
					n [a]:	6
					$\bar{x}$ [b]:	176.4
					s [c]:	2.5
					$u(\bar{x})$ [d]	1.0
R1-1	Blank-1		0.00204	14.293	0.00029	
R1-5	Blank-2		0.00220	46.862	-0.00004	
R2-9	Blank-3		0.00210	61.556	-0.00008	
R2-13	Blank-4		0.00220	49.794	-0.00005	
					n [a]:	4
					$\bar{x}$ [b]:	0.00003
					s [c]:	0.00017

a: number of measurements, b: mean, c: standard deviation, d: standard uncertainty of the mean ($s/\sqrt{n}$)

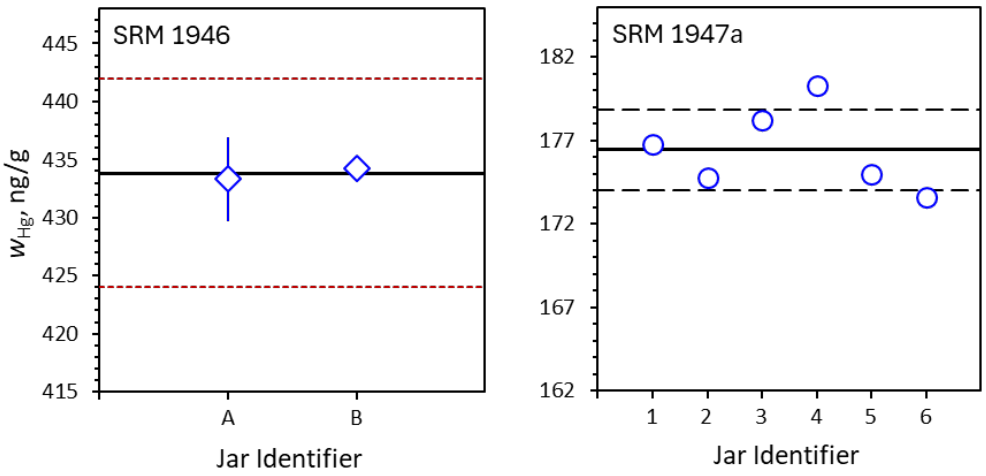

Fig. 6: ID-CV-ICP-MS Results for SRM 1946 and SRM 1947a Samples.

The two diamond symbols (left panel) each represent the mean mass fraction total Hg estimates for three sub-samples from one SRM 1946 jar. The six circle symbols (right panel) each represent the mass fraction total Hg estimate from each SRM 1947a jar. The error bars represent one standard deviation. The thick solid lines represent all-subsample means. The short-dash lines in the left panel bound the certified 95 % level of confidence interval for total Hg in SRM 1946. The long-dash lines in the right panel bound the SRM 1947a (mean ± standard deviation) interval.

The observed total Hg results for SRM 1946 are in excellent agreement with its certified (433 ±9) ng/g 95 % level of confidence interval. This suggests that the SRM 1947a estimated values are unbiased estimates of total Hg.

3.2.7. Uncertainty Budgets

The uncertainty in the ID-CV-ICP-MS mercury measurements of the SRM 1946 and 1947a materials involves contributions from the eleven sources listed in Table 7.

Table 7. Uncertainty Components for ID-CV-ICP-MS Estimated Total Hg in SRMs 1946 and 1947a

Source	Symbol	Basis
Sample replication	$u(r_{sample})$	Standard uncertainty of the mean for n_1 replicate samples.
Spike calibration	$u(r_{spike})$	Standard uncertainty of the mean of n_2 spike calibration mixtures.
Mass of ^{201}Hg added	$u(m_{201Hg})$	The standard uncertainty from the Certificate of Analysis for SRM 3133 is: $u = U_{95}/k$ = 0.040/2.183 = 0.018 ng/g. This propagates to its dilutions as 100*u/10.004 ≈ 0.2 %.
Mass measurement of sample aliquot	$u(m_{sample})$	Measurement variability due to weighing on a four-place balance, estimated as 0.1 %.
Natural/spike atomic weight ratio	$u(K)$	Uncertainty of the IUPAC atomic weight for Hg divided by the atomic weight of the spike determined by isotopic measurements, estimated at 0.0005 %.
Abundance of ^{202}Hg in spike	$u(A_s)$	Uncertainty in spike isotopic composition and relative impact on the measurement of Hg by ID-MS, estimated at 1.02 % for SRM 1946 and 0.99 % for SRM 1947a.
Abundance of ^{201}Hg in spike	$u(B_s)$	Uncertainty in spike isotopic composition and relative impact on the measurement of by reverse ID-MS, estimated at 0.62 % for SRM 1946 and 0.61 % for SRM 1947a.
Abundance of ^{202}Hg in the sample	$u(A)$	Uncertainty of the IUPAC isotopic composition and relative impact on the measurement of Hg by ID-MS. Estimated at 0.02 %.
Abundance of ^{201}Hg in the sample	$u(B)$	Uncertainty of the IUPAC isotopic composition and relative impact on the measurement of Hg by ID-MS. Estimated at 0.02 %.
^{201}Hg/^{202}Hg ratio measurement	$u(R)$	Uncertainty of the dead-time corrected ICP-MS isotope ratio measurements based on pooled standard deviation of approximately 500 ratio measurement points and subtraction of the instrument blank counts on each isotope. Estimated at 0.75 %.
Mass discrimination correction	$u(F)$	Uncertainty of the correction factor (T/E) for the instrument mass bias/mass discrimination and the impact on the measured mass fraction of Hg using ID-MS approach. Estimated at 0.75 %.

The over-all total Hg standard uncertainty for the fish tissue measurements combines these uncertainty sources in quadrature:

$$u(w_{\mathrm{Hg}}) = \sqrt{\begin{array}{c} u^2(r_{\mathrm{sample}}) + u^2(r_{\mathrm{spike}}) + u^2(m_{201\mathrm{Hg}}) + u^2(m_{\mathrm{sample}}) + u^2(K) \\ + u^2(A_{\mathrm{s}}) + u^2(B_{\mathrm{s}}) + u^2(A) + u^2(B) + u^2(R) + u^2(F) \end{array}} \quad (6)$$

The estimated values for these components and the 95 % level of confidence expanded uncertainties for the SRM 1946 and 1947a ID-CV-ICP-MS measurements are presented in Table 8.

Table 8. Uncertainty Budget for ID-CV-ICP-MS Total Hg in SRMs 1946 and 1947a.

	SRM 1946		SRM 1947a	
Source	u_i	DF	u_i	DF
Sample replication	1.0	5	1.0	5
Spike calibration	0.9	3	0.4	3
Mass of ^{201}Hg added	0.8	11.8	0.3	11.8
Mass measurement of sample aliquot	0.4	> 60	0.2	> 60
Natural/spike atomic weight ratio	0.002	> 60	0.001	> 60
Abundance of ^{202}Hg in spike	4.4	> 60	1.7	> 60
Abundance of ^{201}Hg in spike	2.7	> 60	1.1	> 60
Abundance of ^{202}Hg in the sample	0.1	> 60	0.04	> 60
Abundance of ^{201}Hg in the sample	0.1	> 60	0.04	> 60
^{201}Hg/^{202}Hg ratio measurement	3.3	> 60	1.3	> 60
Mass discrimination correction	3.3	> 60	1.3	> 60
Combined standard uncertainty	7.0		3.0	
Student's t 95 % coverage factor	2.0		2.0	
95 % level of confidence expanded uncertainty	13.9		5.9	

3.2.8. Metrological Traceability

The measured total Hg mass fraction is metrologically traceable to the SI through use of SRM 3133 Mercury Standard Solution (Lot #160921) as the calibrant for the isotope dilution spike calibration.

3.3. Comparison of DC-AAS and ID-CV-ICP-MS Results

The DC-AAS and IC-CV-ICP-MS measurement results are in good agreement. The combination of the results are seen in Table 9 and the comparison is seen in Fig. 7.

Table 9: Combination of Mercury (Hg) in SRM 1947a

	DC-AAS			ID-CV-ICP-MS			Combined		
Analyte	n_m[g]	Value[h]	SD[i]	n_m[g]	Value[h]	SD[i]	n_m[g]	Value[h]	SD[i]
Mercury	6	176.5	2.5	12	173.3	3.9	2	174.9	2.2

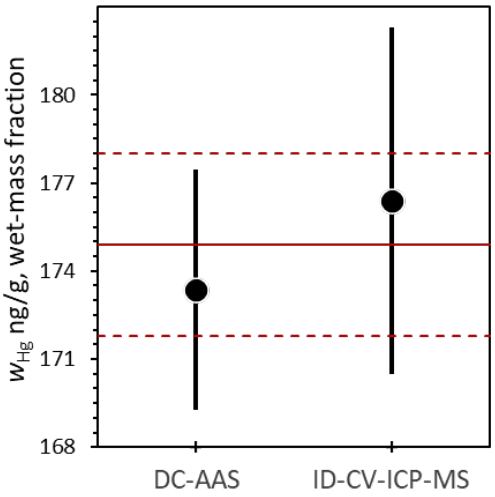

Fig. 7. Comparison of DC-AAS and ID-CV-ICP-MS Hg Mass Fraction Results for SRM 1947a Samples.

The symbol to the left represents the mean wet-mass fraction of Hg in SRM 1947a as determined using DC-AAS; the symbol to the right represents the mean value as determined using IC-CV-ICP-MS. The error bars represent approximate 95 % level of confidence expanded uncertainties on the mean values. The solid horizontal line represents the mean of the two sets of measurements; the dotted lines bracket the approximate 95 % confidence interval about mean.

4. Persistent Organic Pollutants (POPs)

Persistent organic pollutants (POPs) are chemically stable compounds that resist degradation, allowing them to remain in the environment for decades. Their persistence enables long-range transport and accumulation in the tissues of living organisms, creating risks for both human health and ecosystems. POPs are toxic and have been associated with cancer, neurological impairment, thyroid disruption, and reproductive disorders [13, 14]. This study focuses on measurements of polychlorinated biphenyls (PCBs), chlorinated pesticides, and polybrominated diphenyl ethers (PBDEs). Although many of these substances have been banned or are being phased out, global monitoring continues to track their levels in wildlife such as fish, marine mammals, and birds to evaluate bioaccumulation and ecological impact.

PCBs are a group of synthetic organic chemicals consisting of carbon, hydrogen, and chlorine atoms. They were widely used in the past as insulators and coolants in electrical equipment, such as transformers and capacitors, as well as in other applications like pesticides, adhesives, and flame retardants. PBDEs are a class of chemicals consisting of two phenyl rings bonded by an ether linkage, with varying numbers of bromine atoms attached. They have been used as flame retardants in a wide range of products, including textiles, furniture, and mattresses. They have also been added to electronics, automotive interiors, and building materials. Chlorinated pesticides are a class of chlorine containing compounds intended to control pests, specifically insects.

The POPs in SRM 1947a were determined in two measurement campaigns. The first, designated “Method 1”, extracted samples with dichloromethane (DCM) and used SRM 1947 as the control material. The second, designated “Method 2”, extracted samples with a hexane:acetone mixture and used SRM 1946 as the control material. Both measurement methods evaluated the extracts with GC-MS using two separation columns (30 m XLB and 10 m DB-5) and one or both electron impact (EI) and electron capture negative chemical ionization (NCI) detection modes.

4.1. Materials

Measurement control materials used were NIST SRM 1947 for Method 1 and NIST SRM 1946 for Method 2. Calibrants were prepared using SRMs 2257 PBDE Congeners in 2,2,4-Trimethylpentane [15], 2258 BDE 209 in 2,2,4-Trimethylpentane [16], 2259 Polychlorinated Biphenyl Congeners in 2,2,4-Trimethylpentane [17], 2261 Chlorinated Pesticides in Hexane [18], and 2275 Chlorinated Pesticide Solution-II in 2,2,4-Trimethylpentane [19]. Isotopically labeled internal standards were purchased from Wellington Laboratories Inc. (Guelph, Ontario, Canada), Cambridge Isotope Laboratories, Inc. (Tewksbury, MA, USA), AccuStandard. Inc. (New Haven, CT, USA), and Chiron AS (Trondheim, Norway). Solvents used throughout the processes were dichloromethane (DCM), hexane, iso-octane, and acetone.

4.2. Calibration Preparation

Calibrants were prepared by gravimetrically combining NIST SRMs 2257, 2258, 2259, 2261, and 2275. The target masses ranged from approximately (0.143 to 7850) ng of PCBs, (1.41 to

410) ng of chlorinated pesticides, and (0.544 to 944) ng of PBDEs. The components of the calibration solution are listed in Table 10.

Table 10. Components of the Calibration Mixture Prepared from NIST SRMs.

SRM	Compound	SRM	Compound	SRM	Compound	SRM	Compound	SRM	Compound
2257	PBDE 17	2257	PBDE 196	2259	PCB 95	2259	PCB 159	2259	PCB 200
2257	PBDE 25	2257	PBDE 197+204	2259	PCB 99	2259	PCB 163	2259	PCB 201
2257	PBDE 28	2257	PBDE 198	2259	PCB 101	2259	PCB 165	2259	PCB 202
2257	PBDE 30	2257	PBDE 203	2259	PCB 105	2259	PCB 166	2259	PCB 205
2257	PBDE 47	2257	PBDE 206	2259	PCB 106	2259	PCB 167	2259	PCB 206
2257	PBDE 49+71	2257	PBDE 208	2259	PCB 109	2259	PCB 169	2259	PCB 207
2257	PBDE 66	2258	PBDE 209	2259	PCB 110	2259	PCB 170	2259	PCB 208
2257	PBDE 74	2259	PCB 79	2259	PCB 112	2259	PCB 172	2259	PCB 209
2257	PBDE 75	2259	PCB 8	2259	PCB 114	2259	PCB 174	2261	HCB
2257	PBDE 85+155	2259	PCB 18	2259	PCB 118	2259	PCB 175	2261	Heptachlor
2257	PBDE 97+118	2259	PCB 28	2259	PCB 119	2259	PCB 176	2261	2,4’-DDE
2257	PBDE 99+116	2259	PCB 29	2259	PCB 121	2259	PCB 177	2261	4,4’-DDE
2257	PBDE 100	2259	PCB 31	2259	PCB 126	2259	PCB 178	2261	2,4’-DDT
2257	PBDE 101	2259	PCB 44	2259	PCB 127	2259	PCB 180	2261	Mirex
2257	PBDE 119	2259	PCB 45	2259	PCB 128	2259	PCB 183	2261	γ-HCH
2257	PBDE 138	2259	PCB 49	2259	PCB 130	2259	PCB 185	2261	2,4’-DDD
2257	PBDE 139	2259	PCB 52	2259	PCB 153+132	2259	PCB 187	2261	4,4’-DDD
2257	PBDE 153	2259	PCB 56	2259	PCB 137	2259	PCB 188	2261	4,4’-DDT
2257	PBDE 154	2259	PCB 63	2259	PCB 138	2259	PCB 189	2275	Oxychlordane
2257	PBDE 156	2259	PCB 66	2259	PCB 146	2259	PCB 191	2275	α-HCH
2257	PBDE 173+190	2259	PCB 70	2259	PCB 149	2259	PCB 193	2275	β-HCH
2257	PBDE 181	2259	PCB 74	2259	PCB 151	2259	PCB 194	2275	Endrin
2257	PBDE 182	2259	PCB 77	2259	PCB 154	2259	PCB 195		
2257	PBDE 183	2259	PCB 82	2259	PCB 156	2259	PCB 196+203		
2257	PBDE 185	2259	PCB 87	2259	PCB 157	2259	PCB 197		
2257	PBDE 191	2259	PCB 92	2259	PCB 158	2259	PCB 199		

The internal standard (IS) solution was prepared by gravimetrically combining the following compounds: ^{13}C-labeled PCB congeners (28, 52, 118, 153, 180, 194, and 206), ^{13}C-labeled pesticides (HCB, *trans*-chlordane, *trans*-nonachlor, oxychlordane, 4,4'-DDE, 4,4'-DDD, 4,4'-DDT), and labeled PBDE congeners (F-47, F-160, F-208, ^{13}C12-209) and PBDE 104. The composition of the IS solution is described in Table 11.

Table 11. Composition of Internal Standard Mixture.

Compound	Mass Fraction (ng/g)	Compound	Mass Fraction (ng/g)	Compound	Mass Fraction (ng/g)
^{13}C12-PCB 28	226	6'-F-PBDE 47	304	^{13}C6-HCB	269
^{13}C12-PCB 52	253	PBDE 104	253	^{13}C10-oxychlordane	277
^{13}C12-PCB 118	251	4'-F-PBDE 160	271	^{13}C10-*trans*-chlordane	91.3
^{13}C12-PCB 153	252	4'-F-PBDE 208	306	^{13}C10-*trans*-nonachlor	277
^{13}C12-PCB 180	254	^{13}C12-PBDE 209	231	^{13}C12-4,4'-DDE	634
^{13}C12-PCB 194	250			^{13}C12-4,4'-DDD	270
^{13}C12-PCB 206	254			^{13}C12-4,4'-DDT	276

4.3. Sample Preparation

Sorbents used throughout the sample preparation process (e.g., Na_2SO_4 and alumina) were dried at 650 °C and allowed to cool in a desiccator prior to use.

Samples for Method 1 and Method 2 were prepared separately using different jars of SRMs 1947, 1946, and 1947a, but the sampling procedure was the same. Six replicates from one jar of SRM 1947a were extracted alongside three replicates from one jar of control material (SRM 1947 for Method 1 and SRM 1946 for Method 2), six calibrants, and three procedural blanks. Approximately (2.5 to 3) g of material was mixed in a clean 250 mL beaker with approximately (25 to 30) g of Na_2SO_4. The mixtures were allowed to dry for approximately 10 min and then transferred to 33 mL pressurized fluid extraction (PFE) cells. Calibrants were prepared by gravimetrically spiking approximately 1 mL of each into its respective Na_2SO_4 packed PFE cell. Procedural blanks consisted of Na_2SO_4 packed PFE cells with nothing added. All PFE cells, including procedural blanks, were spiked gravimetrically using a gastight syringe with approximately 0.5 mL of the IS solution.

4.3.1. Pressurized Fluid Extraction (PFE)

4.3.1.1. PFE Method 1

All PFE cells were extracted with DCM in an Accelerated Solvent Extractor (Dionex). The extraction cycle conditions were as follows: PFE cell temperature and pressure were 100 °C and 13.79 MPa (2000 pound-force per square inch), respectively, with an equilibration time of 5 min followed by a static time of 5 min. The extraction process consisted of three cycles using one-third of the total solvent volume per cycle. After PFE, extracts were store at -20 °C for at least 8 h, allowed to equilibrate to room temperature, and then reduced in volume to approximately 10 mL under a stream of dry nitrogen gas (N_2) using a Turbovap II (Zymark), and analyzed for total extractable organics as described in Section 4.3.2.

4.3.1.2. PFE Method 2

All PFE cells were extracted with 50:50 v/v hexane and acetone in an Accelerated Solvent Extractor (Dionex). The extraction cycle conditions were as follows: PFE cell temperature and pressure were 100 °C and 13.79 MPa (2000 pound-force per square inch), respectively, with an equilibration time of 5 min followed by a static time of 5 min. The extraction process consisted of three cycles using one-third of the total solvent volume per cycle. After PFE, extracts were store at -20 °C for at least 8 h, allowed to equilibrate to room temperature, and then reduced in volume and solvent-exchanged into DCM to approximately 1 mL under N_2 using a Turbovap II. After solvent exchange into DCM, any excess water on the surface was removed using a pipette prior to size exclusion chromatography.

4.3.2. Total Extractable Organics (TEO)

During Method 1, total extractable organics (TEO) were determined for SRM 1947, SRM 1947a, and blank extracts by gravimetrically transferring approximately 20 % of each extract to respective tared aluminum weighing pans, evaporating for approximately 24 h and reweighing. The TEO values as percent fraction are shown in Table 12.

Table 12. Total Extractable Organics.

Sample ID	Sample Mass (g)	TEO (% fraction)	Sample ID	Sample Mass (g)	TEO (% fraction)
Blank 1	0.00	0.00	SRM 1947a-1	2.43	15.4
Blank 2	0.00	0.00	SRM 1947a-2	2.42	12.5
Blank 3	0.00	0.00	SRM 1947a-3	2.51	13.2
Blank 4	0.00	0.00	SRM 1947a-4	2.67	14.6
SRM 1947-1	2.54	9.96	SRM 1947a-5	2.49	16.1
SRM 1947-2	2.56	14.1	SRM 1947a-6	2.58	16.2
SRM 1947-3	2.49	9.18			

The remaining portion of each extract was further reduced to 1 mL by evaporation under N_2 using a Turbovap II and analyzed using size exclusion chromatography.

4.3.3. Size Exclusion Chromatography (SEC)

High molecular mass compounds were removed from extracts using a size exclusion chromatography (SEC) system (AccuPrep MPS; J2 Scientific) equipped with a PLGel 110 mm × 25 mm i.d.; 10 µm particle size guard column (Polymer Labs) coupled to a 600 mm × 25 mm (10 µm particle size with 100 Å diameter pores) PLGel column (Polymer Labs). Briefly, 1 mL of the extract was injected onto the system. DCM was delivered at 10 mL/min and absorbance was monitored at 254 nm using an internal UV/VIS detector. The first 190 mL fraction, containing high molecular mass compounds, was discarded. The subsequent 82 mL fraction, containing target analytes, was collected.

Method 1: The extracts were solvent-exchanged with *iso*-octane under N_2 using a Turbovap (Biotage) to a final volume of 0.5 mL, and transferred to amber autosampler vials (ASVs).

Method 2: The extracts were solvent-exchanged with 20 % (volume fraction) DCM in hexane using a Turbovap to a final volume of 1 mL in a TurboVap tube.

4.3.4. Solid Phase Extraction (SPE)

Method 1: Activated alumina (50-200 micron; Arcōs Organics, NJ, USA) was partially deactivated by adding 5 % (mass fraction) hexane-rinsed, ultrapure water then packed between two frits in a 3 mL Bond Elut reservoir (Varian, Palo Alto, CA) to approximately 3.9 cm bed height. This amounted to approximately 1.8 g alumina. The SPE cartridges were stored in a sealed desiccator until use and were used the same day they were packed. SPE was carried out using a Rapid Trace automated workstation. Cartridges were conditioned with 6 mL of 50 % (volume fraction) DCM in hexane and 8 mL of hexane at 1.2 mL/min. A 0.5 mL sample was loaded onto each cartridge, followed by 1 mL of hexane that was used to rinse the ASV. The cartridge containing the sample was eluted with 9 mL 35 % (volume fraction) DCM in hexane. Eluants were evaporated in a stream of N_2 using a Turbovap (Biotage), solvent-exchanged with *iso*-octane to a final volume of 0.5 mL and transferred to clean ASVs.

Method 2: Hypersep Amino SPE cartridges with 1000 mg bed weight and 6 mL column capacity were used. SPE was carried out using a manual vacuum manifold. The cartridges were conditioned with 20 mL of 20 % (volume fraction) DCM in hexane at approximately 2 mL/min. A 1 mL sample was loaded onto the cartridge, followed by 1 mL of 20 % (volume fraction) DCM in hexane to rinse the TurboVap tube. The cartridge was eluted with 20 mL 20 % (volume fraction) DCM in hexane into a TurboVap tube. Eluants were evaporated in a stream of N_2 using a Turbovap (Biotage), solvent-exchanged with *iso*-octane to a final volume of 0.5 mL and transferred to clean ASVs.

All extracts were stored at -20 °C when not in use and vortexed prior to analysis.

4.4. Instrumental Analysis

POPs were determined using two gas chromatography mass spectrometry (GC-MS) systems: (1) an Agilent 8890 GC coupled to a 5977B mass spectrometer (MS) with different columns and different ionization modes and (2) an Agilent 7890A GC coupled to a 7000 triple quadrupole MS.

4.4.1. GC-MS with a 30m DB-XLB Column and Electron Impact Ionization (EI) Mode

Both Method 1 and Method 2 sample sets were analyzed on an Agilent 5977B GC-MS using cool-on-column injection (2 µL) onto a 5 m x 0.25 mm Restek Siltek guard column (Bellefonte, PA) connected to a 0.18 mm x 30 m DB-XLB capillary column, 0.18 µm film thickness (Agilent, Palo Alto, CA) set on oven track mode. The GC oven was held at 60 °C for 1.0 min, ramped to 170 °C (25 °C/min), ramped to 270 °C (2 °C/min), ramped to 325 °C (25 °C/min) and held isothermally for 10 min. Total run time for each sample was 67.6 min. Helium was the carrier gas and set at a constant flow rate of 0.8 mL/min. The MS source was operated in electron

impact ionization (EI) mode with selected ion monitoring (SIM). Table 13 lists the monitored ions and approximate retention times.

Table 13. GC-MS Analyte Parameters for a 30m DB-XLB column in EI mode.

Analyte	Quant[a] *m/z*	Qual[b] *m/z*	RT[c] min	Analyte	Quant[a] *m/z*	Qual[b] *m/z*	RT[c] min	Analyte	Quant[a] *m/z*	Qual[b] *m/z*	RT[c] min
PCB 8	152	222	13.96	4,4'-DDE	246	248	30.32	PCB 166	360	362	38.69
α-HCH	219	217	14.18	PCB 154	360	362	30.54	PCB 128	360	362	39.56
^{13}C6-HCB	290	292	14.54	PCB 110	326	328	30.92	PCB 185	394	396	39.65
HCB	284	286	14.54	2,4'-DDD	235	237	30.99	PCB 174	394	396	39.99
γ-HCH	219	217	15.99	PCB 82	326	328	31.63	PCB 167	360	362	40.31
PCB 18	256	258	15.99	PCB 151	360	362	31.63	PCB 202	430	428	40.48
β-HCH	219	217	18.04	PCB 149	360	362	32.45	PCB 177	394	396	40.80
PCB 29	256	258	18.13	PCB 107+109	326	328	32.46	PCB 201	430	428	41.17
PCB 31	256	258	19.33	PCB 106	326	328	33.23	PCB 197	430	428	41.87
^{13}C12-PCB 28	268	270	19.49	2,4'-DDT	235	237	33.42	PCB 156	360	362	42.17
PCB 28	256	258	19.50	^{13}C12-PCB 118	338	340	33.66	PCB 172	394	396	42.32
Heptachlor	272	274	19.65	PCB 118	326	328	33.67	PCB 157	360	362	42.47
PCB 45	292	290	20.30	PCB165	360	362	33.82	^{13}C12-PCB 180	406	408	42.94
^{13}C12-PCB 52	304	302	21.37	PCB 146	360	362	34.42	PCB 180	394	396	42.96
PCB 52	292	290	21.39	^{13}C12-4,4'-DDD	247	249	34.69	PCB 193	394	396	43.12
PCB 49	292	290	21.72	4,4'-DDD	235	237	34.70	PCB 200	430	428	43.15
PCB 44	292	290	22.71	^{13}C12-PCB 153	372	374	34.96	PCB 191	394	396	43.52
PCB 63	292	290	25.73	PCB 114	326	328	34.98	Mirex	272	274	45.15
PCB 95	326	328	25.92	PCB 153+132	360	362	34.99	PCB 170	394	396	45.32
PCB 74	292	290	26.05	PCB 105	326	328	35.76	PCB 199	430	428	45.56
PCB 121	326	328	26.23	PCB 176	394	396	36.07	PCB 196+203	428	430	46.10
PCB 70	292	290	26.25	PCB 137	360	362	36.40	PCB 189	394	396	47.97
PCB 66	292	290	26.54	PCB 127	326	328	36.45	PCB 208	464	466	47.97
2,4'-DDE	246	248	27.19	^{13}C12-4,4'-DDT	247	249	37.22	PCB 207	464	466	48.73
PCB 92	326	328	27.45	4,4'-DDT	235	237	37.24	PCB 195	430	428	48.74
PCB 56	292	290	27.57	PCB 130+138	360	362	37.26	^{13}C12-PCB 194	442	440	50.73
PCB 101	326	328	27.94	PCB 163	360	362	37.37	PCB 194	430	428	50.75
PCB 99	326	328	28.36	PCB 178	394	396	37.50	PCB 205	430	428	51.34
PCB 119+112	326	328	28.96	PCB 158	360	362	37.62	^{13}C12-PCB 206	476	478	53.32
PCB 79	292	290	29.53	PCB 175	394	396	37.99	PCB 206	464	466	53.36
PCB 87	326	328	30.11	PCB 159	360	362	38.22	PCB 209	500	502	55.22
^{13}C12-4,4'-DDE	258	260	30.27	PCB 187+183	394	396	38.24				

a Mass/charge ratio of quantifying ion b Mass/charge ratio of qualifying ion c Peak retention time

The analytes in a 30m DB-XLB column EI mode analysis are displayed in the Fig. 8 exemplar chromatogram.

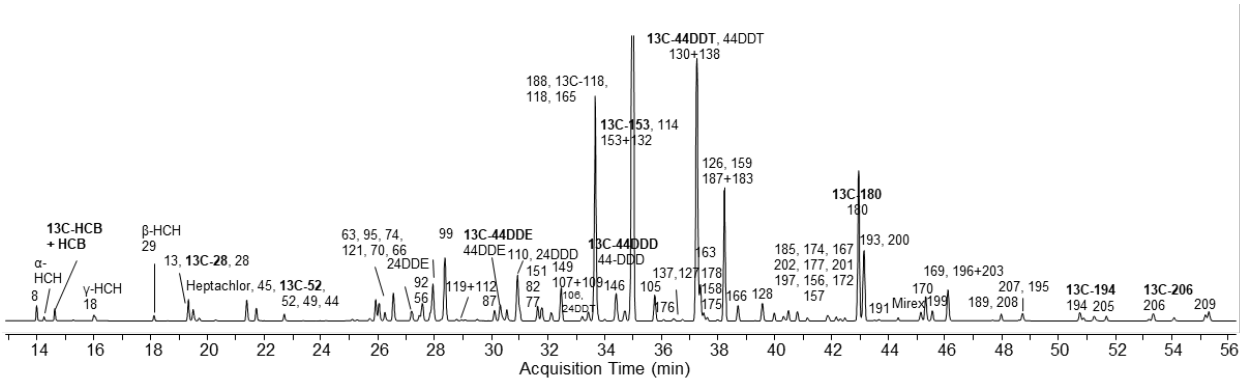

Fig. 8. GC-MS Chromatogram for PCBs and Pesticides with a 30m DB-XLB Column in EI Mode.

PCBs are labeled by number. ^{13}C-labeled internal standards are bolded.

4.4.2. GC-MS with a 30m DB-XLB Column and ENCI mode

The Method 1 sample set was also analyzed on an Agilent 5977B GC-MS using cool-on-column injection (2 µL) onto a 5 m x 0.25 mm Restek Siltek guard column (Bellefonte, PA) connected to a 0.18 mm x 30 m DB-XLB capillary column, 0.18 µm film thickness (Agilent, Palo Alto, CA) set on oven track mode. The GC oven was held at 60 °C for 1.0 min, ramped to 170 °C (25 °C/min), ramped to 270 °C (2 °C/min), then ramped to 325 °C (25 °C/min) and held isothermally for 10 min. Total run time for each sample was 67.6 min. Helium was the carrier gas and the flow rate was held constant at 1.0 mL/min. Methane was used as the reagent gas. The MS source was operated in electron capture negative chemical ionization (ECNI) mode with SIM. The source and quadrupole temperatures were both 150 °C. Table 14 lists the monitored ions and approximate retention times.

Table 14. GC-MS Analyte Parameters for a 30m DB-XLB column in ECNI mode.

Analyte	Quant[a] *m/z*	Qual[b] *m/z*	RT[c] min	Analyte	Quant[a] *m/z*	Qual[b] *m/z*	RT[c] min	Analyte	Quant[a] *m/z*	Qual[b] *m/z*	RT[c] min
α-HCH	255	257	13.08	PBDE 47	79	81	41.59	PBDE 155	79	81	54.91
^{13}C6-HCB	290	292	13.42	PBDE 74	79	81	42.27	PBDE 85	79	81	55.28
HCB	284	286	13.42	PBDE 66	79	81	43.05	PBDE 154	79	81	56.15
γ-HCH	255	257	14.77	PBDE 104	79	81	45.53	PBDE 153	79	81	57.62
β-HCH	255	257	16.74	PBDE 100	79	81	48.73	PBDE 139	79	81	58.11
^{13}C10-oxychlor	360	362	23.33	PBDE 101	79	81	49.12	4F-PBDE 160	79	81	58.36
oxychlordane	350	424	23.36	PBDE 119	79	81	49.53	PBDE 138	79	81	59.09
6F-PBDE 47	79	81	38.35	PBDE 99	79	81	51.05	PBDE 156	79	81	59.69
PBDE 75	79	81	39.07	PBDE 116	79	81	51.88	PBDE 183	79	81	60.55
PBDE 49	79	81	39.82	PBDE 118	79	81	53.03				
PBDE 71	79	81	39.82	PBDE 97	79	81	53.03				

a Mass/charge ratio of quantifying ion b Mass/charge ratio of qualifying ion c Peak retention time

The analytes in a 30m DB-XLB column ECNI mode analysis are displayed in the Fig. 9 exemplar chromatogram.

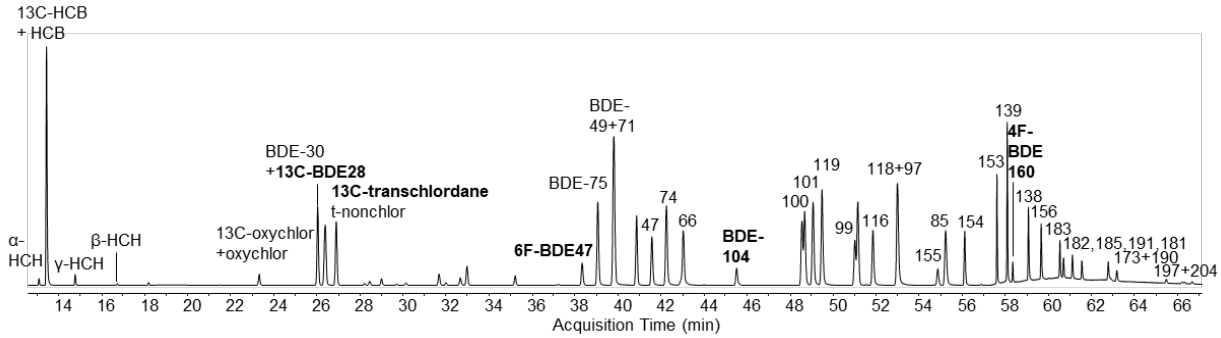

Fig. 9. GC-MS Chromatogram for PCBs and Pesticides with a 30m DB-XLB Column in ECNI Mode.

Peaks labeled with only a number are PBDEs. Internal standards are bolded.

4.4.3. GC-MS with a 10m DB-5MS Column and ENCI mode

Both Method 1 and Method 2 sample sets were analyzed on an Agilent 7000 GC-MS using cool-on-column injection (2 µL) onto a 5 m x 0.25 mm Restek Siltek guard column (Bellefonte, PA) connected to a 0.18 mm x 10 m DB-5MS capillary column, 0.18 µm film thickness (J&W) set on oven track mode. The GC oven was held at 70 °C for 1 min, ramped to 170 °C (40 °C/min), ramped to 305 °C (10 °C/min) and held isothermally for 5 min, then ramped to 325 °C (40 °C/min) and held isothermally for 7 min. Total run time for each sample was 29.5 min. Helium was the carrier gas and the flow was held constant at 0.7 mL/min (Method 1) or 1.4 mL/min (Method 2). Methane was used as the reagent gas. The MS source was operated in ECNI mode in SIM. The transfer line temperature was 280 °C and the source temperature was 250 °C. Table 15 lists the monitored ions and approximate retention times.

Table 15. GC-MS Analyte Parameters for a 10m DB-5 Column in ECNI Mode.

Analyte	Quant[a] *m/z*	Qual[b] *m/z*	RT[c] min	Analyte	Quant[a] *m/z*	Qual[b] *m/z*	RT[c] min	Analyte	Quant[a] *m/z*	Qual[b] *m/z*	RT[c] min
PBDE 17	79	81	7.32	PBDE 99	79	81	11.28	PBDE 191	79	81	15.10
PBDE 25	79	81	7.32	PBDE 116	79	81	11.39	PBDE 181	79	81	15.48
PBDE 33	79	81	7.63	PBDE 118	79	81	11.67	PBDE 173	79	81	15.64
PBDE 28	79	81	7.63	PBDE 97	79	81	11.67	PBDE 190	79	81	15.64
4F-PBDE 47	79	81	8.89	PBDE 85	79	81	12.02	PBDE 197+204	79	81	16.42
PBDE 75	79	81	8.92	PBDE 155	79	81	12.02	PBDE 198	79	81	16.74
PBDE 49	79	81	9.26	PBDE 154	79	81	12.39	PBDE 203	79	81	16.74
PBDE 71	79	81	9.26	PBDE 153	79	81	13.03	PBDE 196	79	81	16.86
PBDE 47	79	81	9.46	PBDE 139	79	81	13.18	PBDE 206	79	81	19.37
PBDE 74	79	81	9.63	4F-PBDE 160	79	81	13.33	PBDE 208	79	81	18.53
PBDE 66	79	81	9.78	PBDE 138	79	81	13.76	4F-PBDE 208	79	81	18.53
PBDE 104	79	81	10.24	PBDE 156	79	81	14.08	^{13}C12-PBDE 209	492	415	22.66
PBDE 100	79	81	10.82	PBDE 183	79	81	14.70	PBDE 209	408	486	22.66
PBDE 101	79	81	10.99	PBDE 182	79	81	14.70				
PBDE 119	79	81	10.99	PBDE 185	79	81	14.70				

a Mass/charge ratio of quantifying ion b Mass/charge ratio of qualifying ion c Peak retention time

The analytes in a 10m DB-5 Column ECNI mode analysis are displayed in the Fig. 10 exemplar chromatogram.

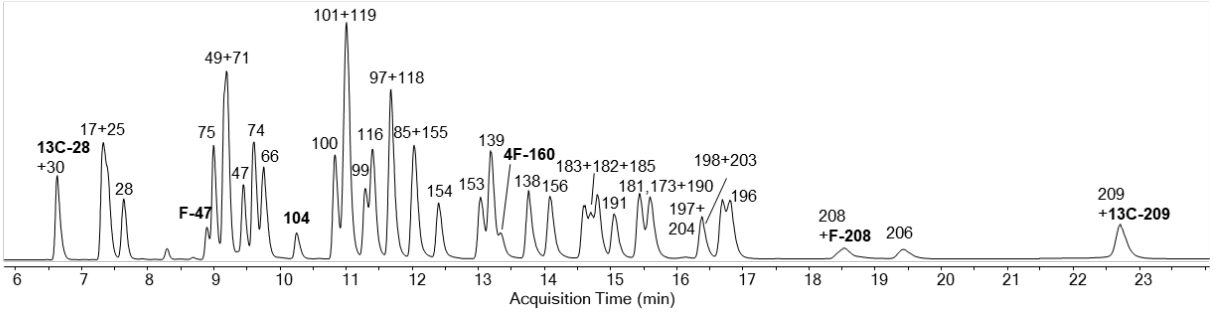

Fig. 10. GC-MS Chromatogram for PBDEs with a 10m DB-5 Column in ECNI Mode.

PBDEs are labeled by number. Internal standards are bolded.

4.5. Measurement Results

Using the Environmental Metrology Measurement Assistant (EMMA) [20], mass fraction for each analyte was calculated using the slope and floating y-intercept of at least a three-point calibration curve that bracketed the peak area ratios observed in the extracts. Results for the Method 1 samples were calculated using two calibration approaches, the first based on the EMMA default parameters using all calibrants and the second based on a curated subset of calibrants that maximized linearity and when appropriate assigned a forced zero y-intercept.

Mass fractions were determined by dividing the calculated mass of each analyte by the extracted sample mass. A compound was considered significantly above the limit of detection (LOD) if the mass of an analyte in the sample was greater than the mean plus three standard deviations of all blanks.

4.5.1. PCBs

A comparison of results obtained for control materials SRM 1946 and SRM 1947 to their respective COA values is shown in Fig. 11. For the majority of PCBs, the results obtained were within acceptable limits, confirming the accuracy of measurements for SRM 1947a. However, for a subset of PCBs (e.g., 56, 63, and 77 in SRM 1946 and 18, 45, and 158 in SRM 1947), the data underwent careful scrutiny prior to being used in value assignment.

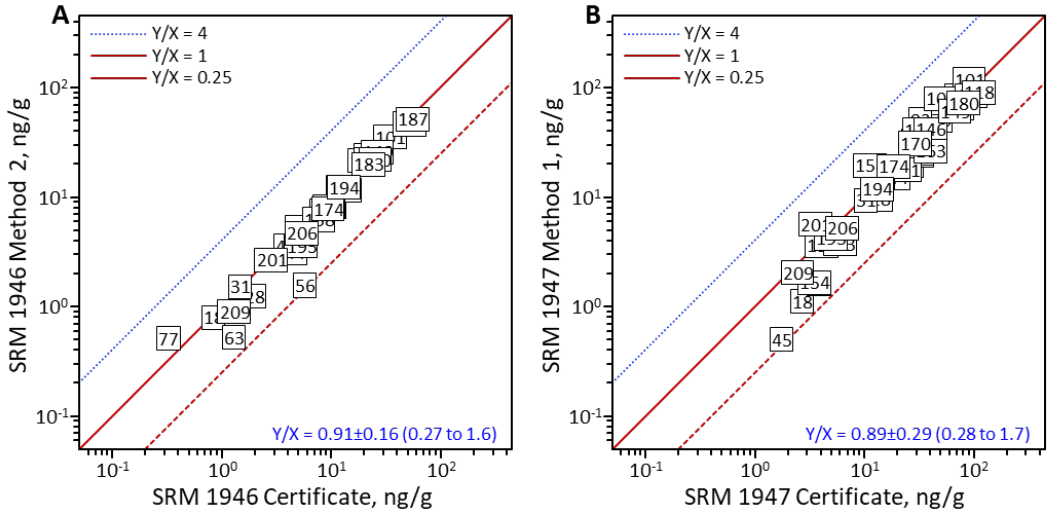

Fig. 11. Comparison of PCB Control Results to COA Values.

Panel A compares the PCB results for SRM 1946 control with the certified and non-certified values listed in the SRM 1946 Certificate of Analysis (COA) [1]; Panel B compares the mean of the PCB results for SRM 1947 control with the certified and non-certified values listed in the SRM 1947 COA [2]. Each labeled box within a panel is centered on the location {COA (X), control (Y)}. The solid diagonal line denotes equality between the two sets of values. The dotted diagonal line denotes Y-results that are a factor-of-four larger than the X-results. The short-dashed diagonal line denotes Y-results that are a factor-of-four smaller than the X-results. The values at the bottom right of the chart summarize the Y/X ratios for the two sets of values.

A comparison of results obtained for SRM 1947a using Method 1 and using Method 2 is seen in Fig. 12. For slightly less than half of the PCBs (45 %) the two methods resulted in similar values. Method 1 had a positive bias over Method 2 for 41 % of the PCBs, and Method 2 had a positive bias over Method 1 for 14 % of the PCBs. For some PCBs, the difference between the methods was significant (e.g. 92, 159, and 201 had greater than 100 % difference) and the data underwent careful scrutiny prior to being used in value assignment.

The method 1, method 2, and combined results for PCBs in SRM 1947a are summarized in Table 16.

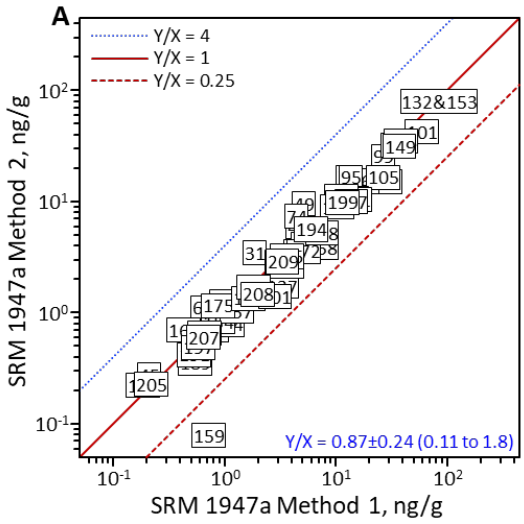

Fig. 12. Comparison of SRM 1947a Method 1 and Method 2 PCB Results.

This figure compares the PCB combined Method 1 results for SRM 1947a with the combined Method 2 results. Each labeled box is centered on the location {Method 1 (X), Method 2 (Y)}. The solid diagonal line denotes equality between the two sets of values. The dotted diagonal line denotes Y-results that are a factor-of-four larger than the X-results. The short-dashed diagonal line denotes Y-results that are a factor-of-four smaller than the X-results. The values at the bottom right of the chart summarize the Y/X ratios for the two sets of values.

Table 16. Method 1, Method 2, and Combined Results for PBDE Congeners in SRM 1947a, ng/g

PCB	Method 1[a]									Method 2[b]			Combined[c]		
	Calibration 1			Calibration 2			Combined								
Congener	n_r[d]	Mean[e]	SD[f]	n_r[d]	Mean[e]	SD[f]	n_c[g]	Value[h]	SD[i]	n_r[d]	Mean[e]	SD[f]	n_m[j]	Value[k]	SD[l]
18				6	0.94	0.15	1	0.94		6	1.248	0.053	2	1.09	0.22
28	6	2.08	0.31	6	2.39	0.32	2	2.23	0.34	6	2.245	0.094	2	2.239	0.009
31	2	1.36	0.46	6	2.05	0.46	2	1.87	0.53	6	3.428	0.064	2	2.7	1.1
44	6	5.1	1.5	6	3.92	0.96	2	4.5	1.4	6	5.90	0.17	2	5.21	0.98
45	2	0.219	0.078	6	0.208	0.086	2	0.211	0.079	6	0.273	0.014	2	0.242	0.044
49	6	4.6	1.8	6	5.7	1.5	2	5.2	1.7	6	9.47	0.36	2	7.3	3.0
52	6	14.7	2.5	6	15.2	2.5	2	14.9	2.4	6	13.87	0.33	2	14.40	0.75
56				6	4.33	0.80	1	4.3		6	3.52	0.15	2	3.92	0.58
63	6	0.53	0.37	6	0.73	0.15	2	0.63	0.29	6	1.107	0.094	2	0.87	0.34
66	6	19.8	4.8	6	21.2	4.9	2	20.5	4.7	6	15.20	0.94	2	17.8	3.7
70	6	15.7	4.8	6	9.7	2.7	2	12.7	4.9	6	16.55	0.65	2	14.6	2.7
74	6	4.9	1.8	6	4.0	1.4	2	4.5	1.6	6	7.31	0.29	2	5.9	2.0
77										6	0.999	0.063	1	1.0	
79	6	1.15	0.49	6	0.54	0.16	2	0.84	0.47	6	0.705	0.041	2	0.775	0.099
82	3	1.09	0.41	6	0.73	0.14	2	0.85	0.30	6	0.913	0.049	2	0.881	0.045
87	6	13.0	4.3	6	18.8	4.1	2	15.9	5.0	6	10.97	0.36	2	13.4	3.5
92	6	29.5	5.3	6	32.1	5.4	2	30.8	5.3	6	14.98	0.71	2	23	11
95	6	13.1	1.9	6	14.2	2.5	2	13.7	2.2	6	16.48	0.62	2	15.1	2.0
99	6	25.9	4.5	6	27.0	4.3	2	26.5	4.2	6	25.5	1.3	2	25.98	0.68
101	6	63.5	11.7	6	55.7	9.7	2	60	11	6	42.2	2.1	2	51	12
105	6	28.1	6.8	6	25.2	5.2	2	26.6	5.9	6	16.50	0.96	2	21.6	7.2
106	6	0.82	0.24	6	0.93	0.23	2	0.88	0.23				1	0.88	
110	6	34.7	6.9	6	36.9	6.1	2	35.8	6.3	6	31.8	1.3	2	33.8	2.8
112										6	2.082	0.073	1	2.1	
114	6	1.02	0.28	6	1.11	0.26	2	1.06	0.26	6	0.784	0.088	2	0.92	0.20
118	6	37.9	7.5	6	38.3	7.4	2	38.1	7.1	6	35.0	1.6	2	36.5	2.2
119										6	2.315	0.097	1	2.3	
127				1	0.18		1	0.18		6	0.221	0.014	2	0.202	0.026
128	6	13.3	3.2	6	14.6	2.8	2	14.0	2.9	6	10.63	0.50	2	12.3	2.3
130										6	5.41	0.25	1	5.4	
137	6	3.23	0.87	6	3.34	0.76	2	3.28	0.78	6	1.72	0.20	2	2.5	1.1

PCB	Method 1[a]									Method 2[b]			Combined[c]		
	Calibration 1			Calibration 2			Combined								
Congener	n_r[d]	Mean[e]	SD[f]	n_r[d]	Mean[e]	SD[f]	n_c[g]	Value[h]	SD[i]	n_r[d]	Mean[e]	SD[f]	n_m[j]	Value[k]	SD[l]
146	6	20.3	4.1	6	22.4	4.0	2	21.4	4.0				1	21	
149	6	36.5	7.7	6	37.8	7.6	2	37.2	7.3	6	31.3	1.4	2	34.2	4.1
151	6	14.3	3.0	6	15.2	2.6	2	14.7	2.7	6	10.38	0.50	2	12.6	3.1
154				6	0.88	0.16	1	0.88		6	0.823	0.055	2	0.851	0.040
156	6	5.5	1.1	6	5.8	1.1	2	5.7	1.1	6	4.12	0.16	2	4.9	1.1
157	6	1.23	0.28	6	1.36	0.28	2	1.30	0.28	6	1.029	0.047	2	1.16	0.19
158	6	7.2	1.8	6	7.6	1.8	2	7.4	1.7	6	3.86	0.32	2	5.6	2.5
159	6	0.68	0.16	6	0.76	0.16	2	0.72	0.15	6	0.078	0.008	2	0.40	0.45
163	6	19.9	6.3	6	23.0	5.7	2	21.5	6.0				1	21	
165	6	16.8	3.3	6	16.9	3.3	2	16.9	3.1				1	17	
166	2	0.39	0.19	6	0.442	0.095	2	0.43	0.11	6	0.695	0.049	2	0.56	0.19
167	6	3.55	0.72	6	3.77	0.70	2	3.66	0.69	6	2.59	0.15	2	3.12	0.75
170	6	10.7	2.9	6	11.9	2.5	2	11.3	2.7	6	11.05	0.48	2	11.15	0.15
172	6	4.9	1.3	6	5.5	1.3	2	5.2	1.3	6	3.56	0.21	2	4.4	1.2
174	6	9.7	2.6	6	10.7	2.8	2	10.2	2.6	6	8.88	0.34	2	9.53	0.93
175	5	0.82	0.32	6	0.91	0.21	2	0.87	0.26	6	1.158	0.058	2	1.01	0.20
176	6	0.48	0.17	6	0.85	0.18	2	0.66	0.26	6	0.657	0.013	2	0.660	0.005
177	6	14.9	4.1	6	12.6	2.9	2	13.8	3.6	6	9.93	0.42	2	11.8	2.7
178	6	7.4	2.2	6	7.6	1.7	2	7.5	1.9	6	5.20	0.21	2	6.4	1.6
180	6	36.2	6.7	6	36.7	6.7	2	36.4	6.4				1	36	
183										6	10.63	0.47	1	11	
185	6	1.64	0.49	6	1.65	0.44	2	1.65	0.44	6	1.348	0.043	2	1.50	0.21
187										6	29.7	1.2	1	30	
189	6	0.544	0.085	6	0.534	0.087	2	0.539	0.082	6	0.351	0.016	2	0.44	0.13
191	6	0.43	0.14	6	0.63	0.14	2	0.53	0.17	6	0.418	0.022	2	0.474	0.078
193	6	1.55	0.26	6	1.64	0.26	2	1.59	0.25				1	1.6	
194	6	6.04	0.99	6	5.95	0.99	2	6.00	0.94	6	5.62	0.15	2	5.81	0.27
195	6	1.57	0.39	6	2.04	0.46	2	1.81	0.48	6	1.685	0.078	2	1.746	0.086
196										6	9.2	1.4	1	9.2	
196										6	9.2	1.4	1	9.2	
197	4	0.465	0.088	6	0.65	0.15	2	0.58	0.16	6	0.486	0.051	2	0.532	0.065
199	6	13.2	3.5	6	9.7	2.2	2	11.4	3.3	6	9.78	0.46	2	10.6	1.2
201	6	2.50	0.65	6	3.17	0.65	2	2.84	0.71	6	1.395	0.055	2	2.1	1.0
202	6	2.46	0.96	6	4.12	0.81	2	3.3	1.2	6	2.86	0.12	2	3.07	0.30

PCB	Method 1[a]									Method 2[b]			Combined[c]		
	Calibration 1			Calibration 2			Combined								
Congener	n_r[d]	Mean[e]	SD[f]	n_r[d]	Mean[e]	SD[f]	n_c[g]	Value[h]	SD[i]	n_r[d]	Mean[e]	SD[f]	n_m[j]	Value[k]	SD[l]
205	4	0.211	0.050	6	0.226	0.057	2	0.220	0.052	6	0.226	0.013	2	0.223	0.004
206	6	3.73	0.55	6	3.57	0.56	2	3.65	0.54	6	3.208	0.069	2	3.43	0.31
207	6	0.55	0.13	6	0.75	0.16	2	0.65	0.17	6	0.595	0.030	2	0.622	0.039
208	6	2.13	0.37	6	1.84	0.34	2	1.99	0.37	6	1.460	0.075	2	1.72	0.37
209	6	3.43	0.50	6	3.16	0.57	2	3.30	0.53	6	2.88	0.10	2	3.09	0.29
106 + 109										6	5.40	0.24	1	5.4	
107 + 109	6	7.0	1.1	6	7.1	1.0	2	7.1	1.0				1	7.1	
112 + 119	6	4.43	0.91	6	4.86	0.92	2	4.65	0.90				1	4.6	
130 + 138	6	62.1	9.9	6	59.3	9.8	2	60.7	9.5				1	61	
132 + 153	6	79.8	17.0	6	89	17	2	84	17	6	78.9	4.1	2	81.6	3.9
138 + 163										6	70.8	3.7	1	71	
146 + 165										6	13.52	0.59	1	14	
180 + 193										6	34.8	1.4	1	35	
183 + 187	6	34.4	8.4	6	39.5	8.3	2	36.9	8.4				1	37	
196 + 203	6	8.1	2.8	6	10.2	2.3	2	9.2	2.7				1	9.2	

a Results for Method 1 extracted samples separated-detected using a 30 m XLB column in EI mode.
b Results for Method 2 extracted samples separated-detected using a 30 m XLB column in EI mode.
c Combination of Method 1 and the mean of Method 2 results.
d The number of replicates with values above background.
e The mean of the replicates with values above background.
f The standard deviation of the replicates with values above background.
g The number of calibrations yielding one or more results above background.
h When both calibrations yielded a result above background, the mean of the two means.
When only one calibration yielded a result above background, the mean of that calibration.
i The standard deviation of the calibration means.
j The number of Methods yielding one or more results above background.
k When both Methods yielded a result above background, the mean of the two means.
When only one Method yielded a result above background, the value of that Method.
l The standard deviation of the Method values.

An interesting comparison is the difference between PCB values in the replacement materials SRM 1947a (from Lake Ontario in 2021) to the original materials, SRM 1946 and SRM 1947 (from Lake Superior and Lake Michigan, respectively, in 1997) as seen in Fig. 13. Of the 68 PCBs measured in both SRM 1947a and SRM 1946, 24 were determined to be at least 30 % lower in SRM 1947a and 27 were determined to be at least 30 % higher in SRM 1947a. PCBs 45, 82, 56, 92, 159, and 209 were > 80 % higher in SRM 1947a. Of the 68 PCBs measured in both SRM 1947a and SRM 1947, 65 were determined to be at least 30 % lower in SRM 1947a and only one (PCB 209) was at least 30 % higher in SRM 1947a.

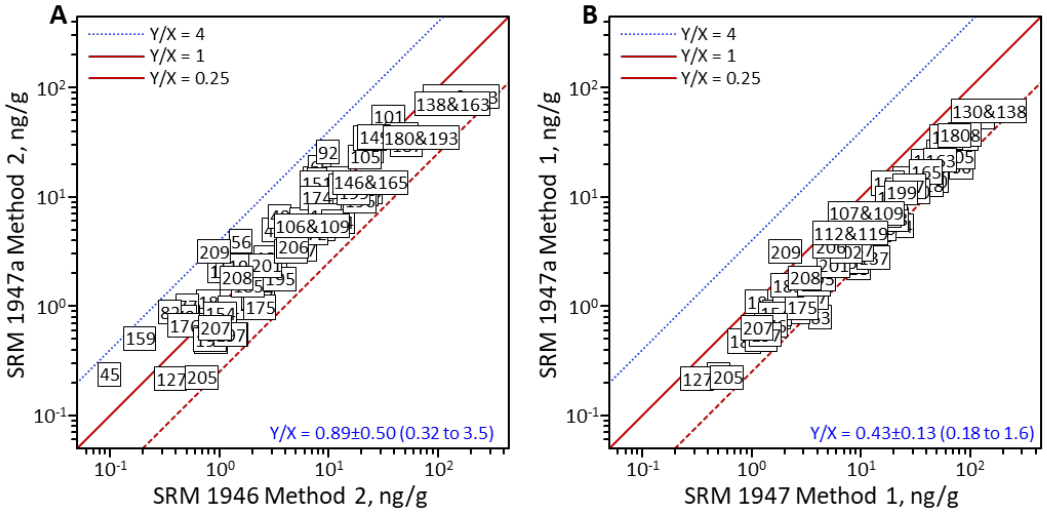

Fig. 13. Comparison of SRM 1946 and 1947 PCB Compositions with SRM 1947a.

Panel A compares the PCB composition of SRM 1946 control with that of SRM 1947a; Panel B compares the PCB composition of SRM 1947 control with that of SRM 1947a. Each labeled box within a panel is centered on the location {control (X), SRM 1947a (Y)}. The solid diagonal line denotes equality between the two sets of values. The dotted diagonal line denotes Y-results that are a factor-of-four larger than the X-results. The short-dashed diagonal line denotes Y-results that are a factor-of-four smaller than the X-results. The values at the bottom right of the chart summarize the Y/X ratios for the two sets of values.

4.5.2. PBDEs

A comparison of results obtained for control materials SRM 1946 and SRM 1947 to their respective COA values is shown in Fig. 14. For the majority of PBDEs, the results obtained were within acceptable limits, confirming the accuracy of measurements for SRM 1947a. However, for a subset of PBDEs (e.g., 49 and 99), the data underwent careful scrutiny prior to being used in value assignment.

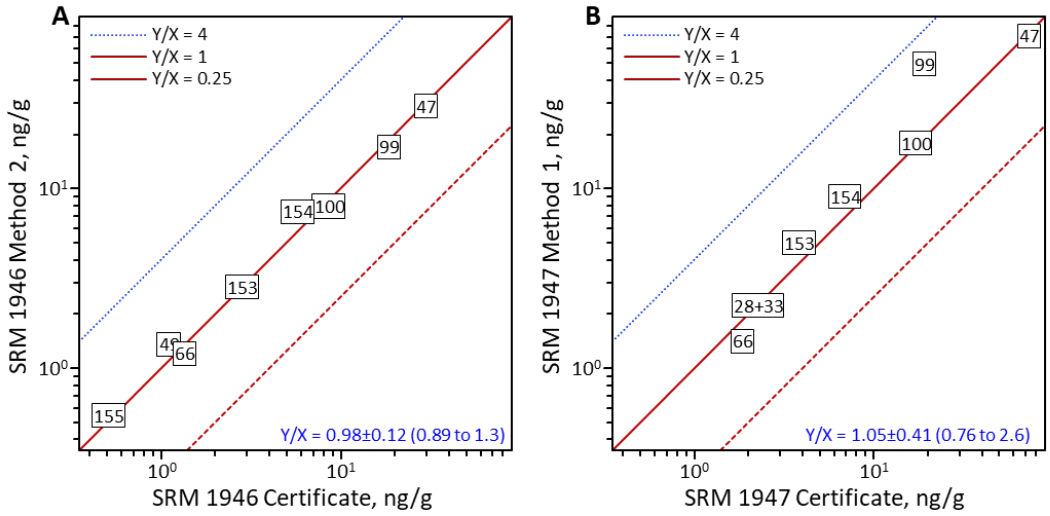

Fig. 14. Comparison of PBDE Control Results to COA Values.

Panel A compares the mean of the PBDE results for SRM 1946 control with the certified and non-certified values listed in the SRM 1946 Certificate of Analysis (COA) [1]; Panel B compares the mean of the PBDE results for SRM 1947 control with the certified and non-certified values listed in the SRM 1947 COA [2]. Each labeled box within a panel is centered on the location {COA (X), control (Y)}. The solid diagonal line denotes equality between the two sets of values. The dotted diagonal line denotes Y-results that are a factor-of-four larger than the X-results. The short-dashed diagonal line denotes Y-results that are a factor-of-four smaller than the X-results. The values at the bottom right of the chart summarize the Y/X ratios for the two sets of values.

A comparison of PBDE results obtained for SRM 1947a using Method 1 and using Method 2 is seen in Fig. 15. The two methods only resulted in similar values for PBDEs 47, 100, 153, 154, and the combination of 49 & 71. For some PBDEs, the difference between the methods was significant (e.g. 30, 99, and 155 had greater than 100 % difference) and the data underwent careful scrutiny prior to being used in value assignment.

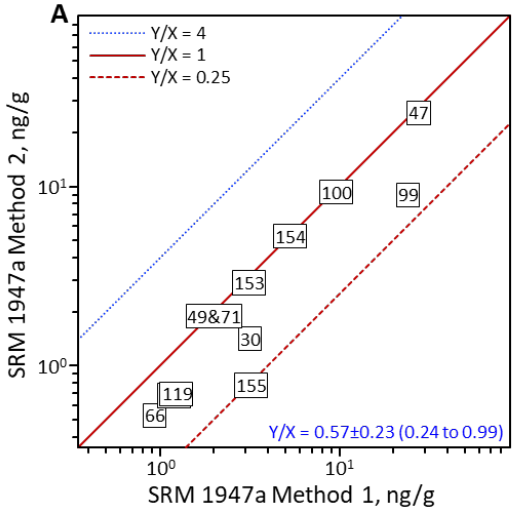

Fig. 15. Comparison of SRM 1947a Method 1 and Method 2 PBDE Results.

This figure compares the combined PBDE Method 1 results for SRM 1947a with the combined Method 2 results. Each labeled box is centered on the location {Method 1 (X), Method 2 (Y)}. The solid diagonal line denotes equality between the two sets of values. The dotted diagonal line denotes Y-results that are a factor-of-four larger than the X-results. The short-dashed diagonal line denotes Y-results that are a factor-of-four smaller than the X-results. The values at the bottom right of the chart summarize the Y/X ratios for the two sets of values.

The method 1 results for PBDEs in SRM 1947a are summarized in Table 17, the method 2 results are summarized in Table 18, and all results are combined and summarized in Table 19.

Table 17. Method 1 Summary Results for PBDE Congeners in SRM 1947a, ng/g.

PBDE	Method 1, 30 m XLB column, ECNI Detection									Method 1, 10 m DB-5 column, ECNI Detection									Combined		
	Calibration 1			Calibration 2			Combined			Calibration 1			Calibration 2			Combined					
Congener	n_r[a]	Mean[b]	SD[c]	n_r[a]	Mean[b]	SD[c]	n_c[d]	Value[e]	SD[f]	n_r[a]	Mean[b]	SD[c]	n_r[a]	Mean[b]	SD[c]	n_c[d]	Value[e]	SD[f]	n_{mg}	Value[h]	SD[i]
30	6	3.60	0.39	6	2.73	0.32	2	3.16	0.57										1	3.16	
47	6	26.67	4.12	6	26.73	4.13	2	26.70	3.93	6	28.72	3.36	6	28.72	3.39	2	28.72	3.22	2	27.71	1.43
66	6	1.35	0.12	6	0.70	0.09	2	1.03	0.35	2	0.63	0.07	2	0.63	0.07	2	0.63	0.06	2	0.83	0.28
74	2	0.77	0.11				1	0.77	0.11										1	0.77	
99				6	24.17	2.44	1	24.2	2.4										1	24.17	
100	6	8.82	0.86	6	8.69	0.85	2	8.75	0.82	6	10.38	1.30	6	10.40	1.32	2	10.39	1.25	2	9.57	1.16
101	6	1.20	0.12				1	1.20	0.12										1	1.20	
119	6	1.24	0.10				1	1.24	0.10										1	1.24	
138	4	1.17	0.17	3	0.73	0.11	2	0.98	0.27										1	0.98	
153	6	3.85	0.25	6	2.95	0.25	2	3.40	0.52	5	2.80	1.42	5	2.80	1.41	2	2.80	1.33	2	3.10	0.42
154	6	5.23	0.38	6	4.99	0.38	2	5.11	0.38	6	5.49	1.24	6	5.48	1.24	2	5.48	1.18	2	5.30	0.26
155				6	3.23	0.20	1	3.23	0.20										1	3.23	
17 + 25										1	4.55		1	4.55		2	4.55	0.00	1	4.55	
28 + 33										6	1.24	0.12	6	1.24	0.12	2	1.24	0.12	1	1.24	
49 + 71				4	1.44	0.12	1	1.44	0.12	6	2.19	0.25	6	2.19	0.25	2	2.19	0.24	2	1.82	0.53
85 + 155	6	2.23	0.17	1	0.79		2	2.03	0.57										1	2.03	
97 + 118	6	1.48	0.14				1	1.48	0.14	1	1.21		1	1.21		2	1.21	0.00	2	1.34	0.19
99 + 116	6	11.97	1.10	6	11.3	1.1	2	11.6	1.1	6	12.42	1.66	6	12.42	1.65	2	12.42	1.58	2	12.02	0.56

a The number of replicate measurement results with values above background.
b The mean of the replicate measurement results with values above background.
c The standard deviation of the replicate measurement results with values above background.
d The number of calibrations yielding one or more results above background.
e When both calibrations yielded a result above background, the mean of the two means.
When only one calibration yielded a result above background, the mean of that calibration.
f The standard deviation of the calibration means.
g The number of Methods yielding one or more results above background.
h When both Methods yielded a result above background, the mean of the two means.
When only one Method yielded a result above background, the value of that Method.

i The standard deviation of the Method values.

Table 18. Method 2 Summary Results for PBDE Congeners in SRM 1947a, ng/g.

PBDE	Separation 1[a]			Separation 2[b]			Combined[c]		
Congener	n_r[d]	Mean[e]	SD[f]	n_r[d]	Mean[e]	SD[f]	N_{sg}	Value[h]	SD[i]
17	6	9.90	0.31				1	9.90	
25	6	2.88	0.17				1	2.88	
28	6	1.02	0.12	6	0.79	0.10	2	0.90	0.16
30	6	1.41	0.06				1	1.41	
47	6	27.72	2.04	6	23.92	1.48	2	25.82	2.61
49				6	1.49	0.11	1	1.49	
66				6	0.53	0.04	1	0.53	
75	6	4.06	0.21				1	4.06	
100	6	10.56	1.43	6	7.96	0.52	2	9.26	1.70
101	5	0.68	0.06				1	0.68	
119	1	0.70					1	0.70	
153	6	3.02	0.16	6	2.78	0.07	2	2.90	0.17
154	6	5.60	0.42	6	4.91	0.13	2	5.25	0.47
155	6	0.78	0.07				1	0.78	
49 + 71	6	1.89	0.24				1	1.89	
99 + 116				6	9.00	0.33	1	9.00	

a Results for Method 2 extracted samples detected using GC-MS with a 30 m XLB column in EI mode.
b Results for Method 2 extracted samples detected using GC-MS with a 10 m DB-5 column in ECNI mode.
c Combination of the Method 2 results from the two separation-detection systems.
d The number of replications yielding results above background.
e The mean of the replicates with values above background.
f The standard deviation of the replicates with values above background.
g The number of separation-detection systems yielding one or more results above background.
h When both separation-detection systems yielded a result above background, the mean of the two means. When only one separation-detection system yielded a result above background, the mean of that system.
i The standard deviation of the separation-detection system means.

Table 19. Combined Results for PBDE Congeners in SRM 1947a, ng/g.

PBDE	Combined			PBDE	Combined			PBDE	Combined		
Congener	n_m[a]	Value[b]	SD[c]	Congener	n_m[a]	Value[b]	SD[c]	Congener	n_m[a]	Value[b]	SD[c]
17	1	9.9		75	1	4.1		155	2	2.0	1.7
25	1	2.9		99	1	24		17 + 25	1	4.5	
28	1	0.90		100	2	9.41	0.22	28 + 33	1	1.2	
30	2	2.3	1.2	101	2	0.94	0.37	49 + 71	2	1.854	0.052
47	2	26.8	1.3	119	2	0.97	0.38	85 + 155	1	2.0	
49	1	1.5		138	1	0.98		97 + 118	1	1.3	
66	2	0.68	0.21	153	2	3.00	0.14	99 + 116	2	10.5	2.1
74	1	0.77		154	2	5.276	0.031				

a The number of Methods yielding one or more results above background.
b When both Methods yielded a result above background, the mean of the two combined values. When only one Method yielded a result above background, the combined value of that Method.
c The standard deviation of the Method values.

An interesting comparison is the difference between PBDE values in the replacement materials SRM 1947a (from Lake Ontario in 2021) to the original materials, SRM 1946 and SRM 1947 (from Lake Superior and Lake Michigan, respectively, in 1997) as seen in Fig. 16. Of the 15 PBDEs measured in both SRM 1947a and SRM 1946, 4 were determined to be at least 30 % lower in SRM 1947a and 5 were determined to be at least 30 % higher in SRM 1947a. PBDEs 30 and 155 were > 100 % higher in SRM 1947a. Of the 17 PBDEs measured in both SRM 1947a and SRM 1947, 11 were determined to be at least 30 % lower in SRM 1947a and no PBDEs were more than 15 % higher in SRM 1947a.

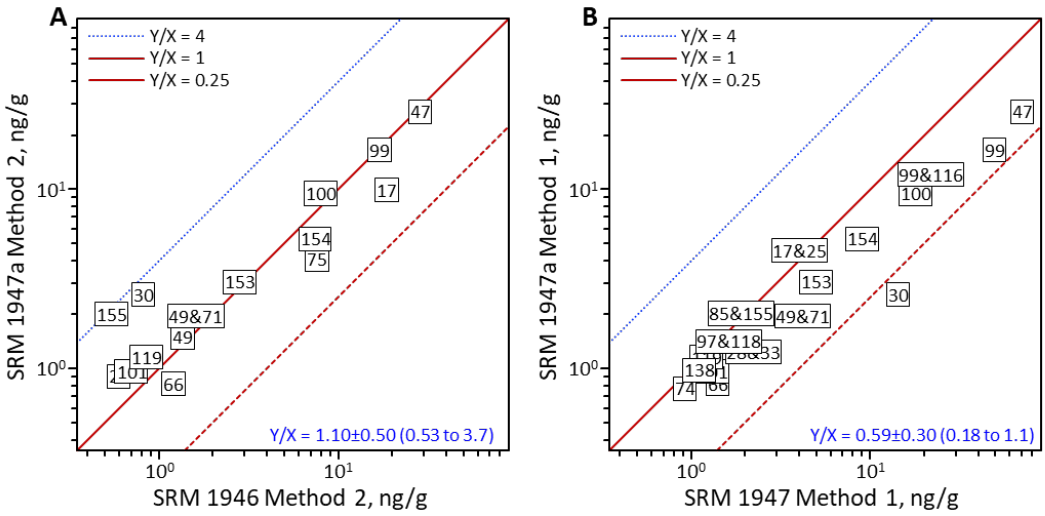

Fig. 16. Comparison of SRM 1946 and 1947 PBDE Compositions with SRM 1947a.

Panel A compares the PBDE composition of SRM 1946 control with that of SRM 1947a; Panel B compares the PBDE composition of SRM 1947 control with that of SRM 1947a. Each labeled box within a panel is centered on the location {control (X), SRM 1947a (Y)}. The solid diagonal line denotes equality between the two sets of values. The dotted diagonal line denotes Y-results that are a factor-of-four larger than the X-results. The short-dashed diagonal line denotes Y-results that are a factor-of-four smaller than the X-results. The values at the bottom right of the chart summarize the Y/X ratios for the two sets of values.

4.5.3. Chlorinated Pesticides

A comparison of results obtained for control materials SRM 1946 and SRM 1947 to their respective COA values is shown in Fig. 17For the majority of chlorinated pesticides, the results obtained were within acceptable limits, confirming the accuracy of measurements for SRM 1947a. However, for a subset of pesticides (e.g., 2,4'-DDD, *cis*-Nonachlor, and *trans*-Chlordane in SRM 1946 and 2,4'-DDE in SRM 1947), the data underwent careful scrutiny prior to being used in value assignment.

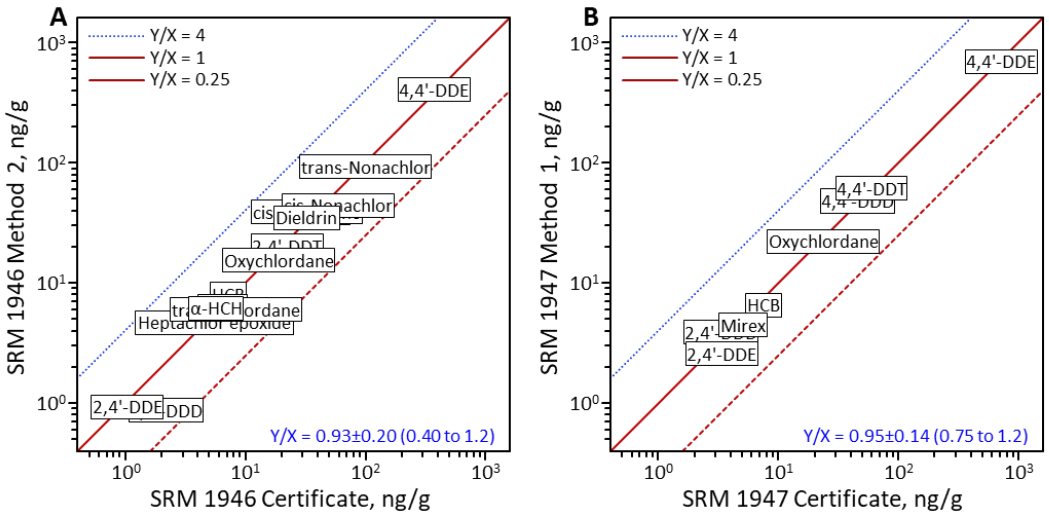

Fig. 17. Comparison of Chlorinated Pesticides Control Results to COA Values.

Panel A compares the chlorinated pesticides results for SRM 1946 control with the certified and non-certified values listed in the SRM 1946 Certificate of Analysis (COA) [1]; Panel B compares the mean of the chlorinated pesticides results for SRM 1947 control with the certified and non-certified values listed in the SRM 1947 COA [2]. Each labeled box within a panel is centered on the location {COA (X), control (Y)}. The solid diagonal line denotes equality between the two sets of values. The dotted diagonal line denotes Y-results that are a factor-of-four larger than the X-results. The short-dashed diagonal line denotes Y-results that are a factor-of-four smaller than the X-results. The values at the bottom right of the chart summarize the Y/X ratios for the two sets of values.

A comparison of the chlorinated pesticides results obtained for SRM 1947a using Method 1 and using Method 2 is seen in Fig. 18. The two methods resulted in similar values for most analytes. For 2,4'-DDE, the difference between the methods was 21 % and for 2,4'DDT the difference was >200 %. These data underwent careful scrutiny prior to being used in value assignment.

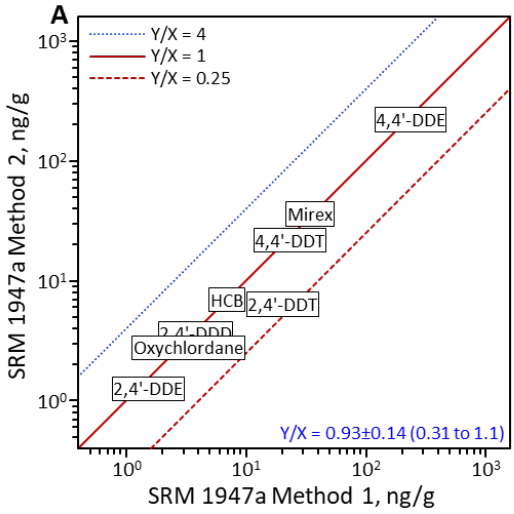

Fig. 18. Comparison of SRM 1947a Method 1 and Method 2 Chlorinated Pesticide Results.

This figure compares the chlorinated pesticide Method 1 results for SRM 1947a with those for the combined Method 2 results. Each labeled box is centered on the location {Method 1 (X), Method 2 (Y)}. The solid diagonal line denotes equality between the two sets of values. The dotted diagonal line denotes Y-results that are a factor-of-four larger than the X-results. The short-dashed diagonal line denotes Y-results that are a factor-of-four smaller than the X-results. The values at the bottom right of the chart summarize the Y/X ratios for the two sets of values.

The method 1 results for chlorinated pesticides in SRM 1947a are summarized in Table 20, the method 2 results are summarized in Table 21, and all results are combined and summarized in Table 22.

Table 20. Method 1 Summary Results for Chlorinated Pesticides in SRM 1947a, ng/g.

	Method 1, 30 m XLB column, EI Detection									Method 1, 30 m XLB column, ECNI Detection										Combined		
	Calibration 1			Calibration 2			Combined			Calibration 1			Calibration 2			Combined					
Analyte	n_r[a]	Mean[b]	SD[c]	n_r[a]	Mean[b]	SD[c]	n_c[d]	Value[e]	SD[f]	n_r[a]	Mean[b]	SD[c]	n_r[a]	Mean[b]	SD[c]	n_c[d]	Value[e]	SD[f]	n_{mg}	Value[h]	SD[i]
HCB	6	6.88	0.97	6	6.98	0.94	2	6.93	0.91	6	6.78	0.22	6	6.92	0.17	2	6.85	0.20	2	6.89	0.06
Oxychlordane										6	2.79	0.69	6	3.79	0.75	2	3.29	0.86	1	3.3	
Mirex	6	34.5	6.8	6	34.0	6.8	2	34.2	6.4										1	34	
2,4'-DDD	6	4.11	0.26	6	3.46	0.21	2	3.78	0.41										1	3.8	
4,4'-DDD	6	46.1	6.4	6	46.2	6.4	2	46.1	6.1										1	46	
2,4'-DDE	6	1.75	0.36	6	1.31	0.36	2	1.53	0.41										1	1.5	
4,4'-DDE	6	236	44	6	235	43	2	235	41										1	235	
2,4'-DDT	6	5.67	0.90	6	34.8	5.7	2	20	16										1	20	
4,4'-DDT	6	22.8	3.8	6	23.7	3.8	2	23.2	3.7										1	23	

a The number of replicates with values above background.
b The mean of the replicates with values above background.
c The standard deviation of the replicates with values above background.
d The number of calibrations yielding one or more results above background.
e When both calibrations yielded a result above background, the mean of the two means.
When only one calibration yielded a result above background, the mean of that calibration.
f The standard deviation of the calibration means.
g The number of separation-detection systems yielding one or more results above background.
h When both separation-detection systems yielded a result above background, the mean of the two means.
When only one system yielded a result above background, the value of that system.
i The standard deviation of the separation-detection system values.

Table 21. Method 2 Summary Results for Chlorinated Pesticides in SRM 1947a, ng/g.

Analyte	n_r[a]	Mean[b]	SD[c]
HCB	6	6.95	0.37
Heptachlor Epoxide	6	1.20	0.05
Oxychlordane	6	2.77	0.13
cis-Chlordane	6	12.85	0.45
trans-Chlordane	6	1.58	0.06
cis-Nonachlor	6	7.60	0.33
trans-Nonachlor	6	21.33	0.83
Dieldrin	6	12.07	0.58
Mirex	6	36.0	2.3
2,4'-DDD	6	3.66	0.17
2,4'-DDE	6	1.26	0.08
4,4'-DDE	6	220.3	5.0
2,4'-DDT	6	6.36	0.80
4,4'-DDT	6	21.63	0.45

a The number of replicate s with values above background.
b The mean of the replicates with values above background.
c The standard deviation of the replicates with values above background.

Table 22. Combined Results for Chlorinated Pesticides in SRM 1947a, ng/g.

Analyte	n_m[a]	Value[b]	SD[c]
HCB	2	5.7	2.4
Heptachlor Epoxide	1	1.2	
Oxychlordane	2	3.0	1.3
cis-Chlordane	1	13	
trans-Chlordane	1	1.6	
cis-Nonachlor	1	7.6	
trans-Nonachlor	1	21	
Dieldrin	1	12	
Mirex	2	28	14
2,4'-DDD	2	3.4	1.4
4,4'-DDD	1	34	
2,4'-DDE	2	1.7	1.3
4,4'-DDE	2	180	96
2,4'-DDT	2	14	13
4,4'-DDT	2	18.2	8.7

a The number of Methods yielding one or more results above background.
b When both Methods yielded a result above background, the mean of the two summary values. When only one Method yielded a result above background, the summary value of that Method.
c The standard deviation of the Method values.

An interesting comparison is the difference between the chlorinated pesticide values in the replacement materials SRM 1947a (from Lake Ontario in 2021) to the original materials, SRM 1946 and SRM 1947 (from Lake Superior and Lake Michigan, respectively, in 1997) as seen in Fig. 19. Of the 14 PCBs measured in both SRM 1947a and SRM 1946, 9 were determined to be at least 30 % lower in SRM 1947a and 3 were determined to be at least 30 % higher in SRM 1947a. 2,4'-DDD and Mirex were greater than 100 % higher in SRM 1947a. Of the 8 pesticides measured in both SRM 1947a and SRM 1947, 4 were determined to be at least 30 % lower in SRM 1947a and one (Mirex) was greater than 150 % higher in SRM 1947a.

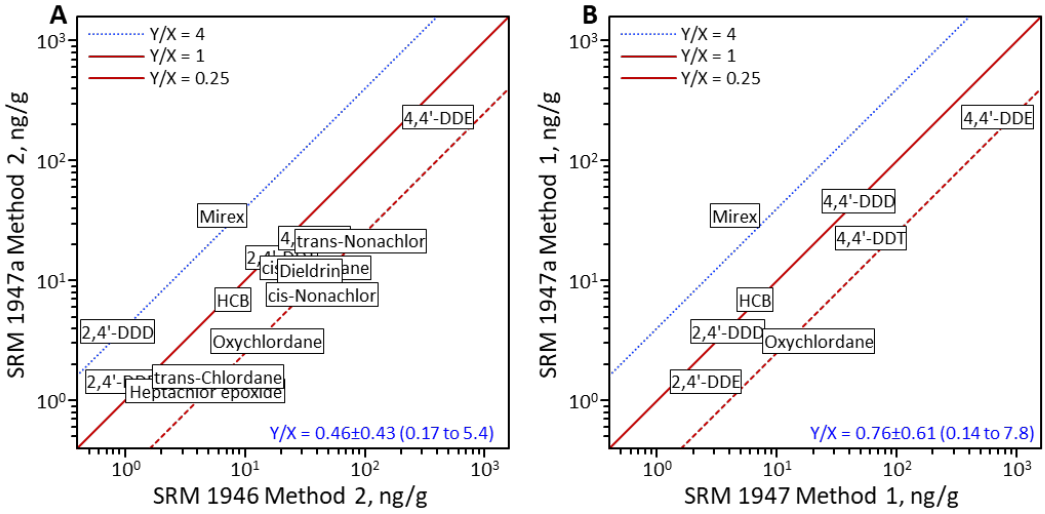

Fig. 19. Comparison of SRM 1946 and 1947 Chlorinated Pesticide Compositions with SRM 1947a.

Panel A compares the chlorinated pesticide Method 1 composition of SRM 1946 control with that of SRM 1947a; Panel B compares the Method 2 composition of SRM 1947 control with that of SRM 1947a. Each labeled box within a panel is centered on the location {control (X), SRM 1947a (Y)}. The solid diagonal line denotes equality between the two sets of values. The dotted diagonal line denotes Y-results that are a factor-of-four larger than the X-results. The short-dashed diagonal line denotes Y-results that are a factor-of-four smaller than the X-results. The values at the bottom right of the chart summarize the Y/X ratios for the two sets of values.

4.6. Metrological Traceability

Mass fractions of POPs determined by the previously-described measurements are metrologically traceable to the SI through the standard reference materials with certified values for the respective POPs (Section 4.2, Table 10).

5. Per- and Polyfluoroalkyl Substances (PFAS) and Homogeneity

Per- and polyfluoroalkyl substances (PFAS) are a class of organic compounds with a carbon chain that is partially or fully fluorinated [21]. The NIST currently provides measurements of PFAS in several SRMs such as SRM 2585 Organic Contaminants in House Dust [22] and SRM 2781 Domestic Sludge [23]. The non-certified reference values delivered by these materials are useful for the development and validation of methods, and the value assignment of PFAS mass fractions in SRM 1947a Great Lakes Fish Tissue will expand the matrix-matched products available to customers.

5.1. PFAS Analysis Method 1

5.1.1. Materials

All solvents were obtained from Thermo Fisher (Optima LC-MS; Waltham, MA). Target PFAS were measured using a stock calibration solution containing 30 PFAS and an isotopically labeled PFAS stock solution containing 19 PFAS. SRM 1947 was used as a quality control material.

This method was used to establish homogeneity of the material. Based on a random sampling scheme, ten jars of SRM 1947a were assigned for homogeneity testing: 1, 102, 816, 1106, 1430, 1546, 1709, 1902, 3904, and 4976.

5.1.2. Calibration Preparation

The calibration solution was gravimetrically diluted to create seven working solutions ranging from (0.1 to 35) ng/g. The isotopically labeled PFAS internal standard (IS) mixture was gravimetrically diluted with methanol to create an internal standard working solution (IS-WS) with mass fractions of approximately 2 ng/g. Target PFAS and associated ISs are listed in Table 23.

Table 23. PFAS Names, Abbreviations, CASRN, and Internal Standards.

Abbreviation	Analyte Name	CASRN	Internal Standard
PFBS	perfluorobutane sulfonic acid	375-73-5	$^{13}C_3$-PFBS
FBSA	perfluorobutanesulfonamide	30334-69-1	$^{13}C_3$-PFBS
PFBA	perfluorobutanoic acid	375-22-4	$^{13}C_4$-PFBA
PFDS	perfluorodecane sulfonic acid	335-77-3	$^{13}C_8$-PFOS
PFDA	perfluorodecanoic acid	335-76-2	$^{13}C_6$-PFDA
PFDoA	perfluorododecanoic acid	307-55-1	$^{13}C_2$-PFDoA
PFHpS	perfluoroheptane sulfonic acid	375-92-8	$^{13}C_3$-PFHxS
PFHpA	perfluoroheptanoic acid	375-85-9	$^{13}C_4$-PFHpA
PFHxS	perfluorohexane sulfonic acid	355-46-4	$^{13}C_3$-PFHxS
PFHxSA	perfluorohexanesulfonamide	41997-13-1	$^{13}C_3$-PFHxS
PFHxA	perfluorohexanoic acid	307-24-4	$^{13}C_5$-PFHxA
PFNS	perfluorononane sulfonic acid	68259-12-1	$^{13}C_8$-PFOS
PFNA	perfluorononanoic acid	375-95-1	$^{13}C_9$-PFNA
PFOS	perfluorooctane sulfonic acid	1763-23-1	$^{13}C_8$-PFOS
PFOSA	perfluorooctanesulfonamide	754-91-6	$^{13}C_8$-PFOSA
PFOA	perfluorooctanoic acid	335-67-1	$^{13}C_8$-PFOA
PFPeS	perfluoropentane sulfonic acid	2706-91-4	$^{13}C_3$-PFBS
PFPeA	perfluoropentanoic acid	2706-90-3	$^{13}C_5$-PFPeA
PFTA	perfluorotetradecanoic acid	376-06-7	$^{13}C_2$-PFTA
PFTriA	perfluorotridecanoic acid	72629-94-8	$^{13}C_2$-PFTA
PFUnA	perfluoroundecanoic acid	2058-94-8	$^{13}C_7$-PFUnA
HFPO-DA	Hexafluoropropylene oxide dimer acid	13252-13-6	$^{13}C_8$-PFOS
NMeFOSAA	N-ethyl perfluorooctanesulfonamide	4151-50-2	d_3-NMeFOSAA
NEtFOSAA	N-methyl perfluorooctanesulfonamide	31506-32-8	d_5-NEtFOSAA
4:2FTS	1H,1H,2H,2H-perfluorohexane sulfonic acid	757124-72-4	$^{13}C_2$-4:2FTS
6:2FTS	1H,1H,2H,2H-perfluorooctane sulfonic acid	27619-97-2	$^{13}C_2$-6:2FTS
8:2FTS	1H,1H,2H,2H-perfluorodecane sulfonic acid	39108-34-4	$^{13}C_2$-8:2FTS
NaDONA	4,8-Dioxa-3H-perfluorononanoic acid, sodium salt	919005-14-4	$^{13}C_8$-PFOS
9Cl-PF3ONS	9-chlorohexadecafluoro-3-oxanonane-1-sulfonic acid	756426-58-1	$^{13}C_8$-PFOS
11Cl-PF3OUnS	11-chloroeicosafluoro-3-oxaundecane-1-sulfonic acid	763051-92-9	$^{13}C_8$-PFOS

5.1.3. Sample Preparation

Calibrants, three blanks (DI water), three replicates (from one jar) of SRM 1947, and ten replicates (one per jar) of SRM 1947a were prepared. Each sample was weighed into 50 mL polypropylene (PP) tubes and spiked with 600 µL of the IS-WS. All tubes were vortexed for 10 sec and allowed to equilibrate for 1.5 hr. Four mL of methanol was added to the samples and the samples were sonicated for 30 min. The samples were centrifuged for 5 min at 753 RCF (2500 rpms). The supernatant was transferred to a precleaned 15-mL PP tube using a glass pipet and cleaned using Supelco Supelclean ENVI-Carb SPE column (3 mL, 250 mg, 120 to 400 mesh; Bellefonte, PA). Briefly, the ENVI-Carb cartridge was rinsed with 7 mL of methanol. After the rinse, a sample collection tube was added to the vacuum manifold, the sample was added to the ENVI-Carb cartridge, and target analytes eluted with 7 mL of methanol. The final eluant from the cartridge was evaporated under nitrogen (35 °C) to approximately 1 mL and transferred to a precleaned autosampler vial for analysis via liquid chromatography tandem mass spectrometry (LC-MS/MS).

5.1.4. Instrumental method

LC-MS/MS analysis was performed using an Agilent Infinity II (Agilent, Santa Clara, CA) connected to an AB Sciex API 5500 Triple Quadrupole Mass Spectrometer (AB Sciex, Framingham, MA). The autosampler tray temperature was set to the ambient air temperature, roughly 25 °C. The mobile phases consisted of 10 mmol/L ammonium acetate in laboratory deionized water (A) and 10 mmol/L ammonium acetate in HPLC grade methanol (B) with a flow rate of 0.350 mL/min and initial composition of 100 % A, 0 % B. The initial mobile phase was equilibrated at this composition for at least 15 min prior to injection. After the 10 µL injection, the mobile phase was changed to 65 % A, 35 % B over 3 min, then changed to 0 % A and 100 % B over the next 22 minutes and held at this composition for 7 min before returning to initial conditions over the next 13 min. A retention column was placed before the pumps (Eclipse Plus C18, 4.6 mm i.d., 50 mm, 5 µm particle size) to separate instrumental contamination. Chromatographic separation was achieved using a Zorbax Diol (4.6 mm i.d., 12.5 mm, 6 µm particle size) guard column attached to an Agilent InfinityLab Poroshell 120 EC-C18 column (4.6 mm i.d., 100 mm, 2.7 µm particle size) column, maintained at ambient air temperature for the entire run. Mass spectrometric detection was performed in electrospray ionization (ESI) in both positive (+) and negative (-) modes. Parameters were Curtain Gas: 20, Collision Gas: 9, Temperature: 350 °C, Ion Source Gas 1: 15, and Ion Source Gas 2: 0 for both modes. The IonSpray voltage was 4500 for (+) mode and -4500 for (-) mode.

5.1.5. Perfluorobutane sulfonamide

Perfluorobutanesulfonamide (FBSA), a short-chain per- and polyfluoroalkyl substance (PFAS), was detected in both SRM 1947 and SRM 1947a. Due to its small molecular size and the limitation of monitoring only a single MS/MS transition, its presence in SRM 1947a remained uncertain. Given its short-chain structure, FBSA has a low potential for bioaccumulation, and longer-chain analogs (perfluorohexanesulfonamide and perfluorooctanesulfonamide) were not detected in either material. To confirm the presence or absence of FBSA, high-resolution mass spectrometry (HRMS) was employed.

Sample extracts were analyzed via flow injection using a Vanquish UPLC system coupled to an Orbitrap Fusion Lumos Tribrid mass spectrometer (ThermoFisher Scientific). A 5 µL reconstituted sample was injected at 350 µL/min using a 50:50 mixture of 10 mmol/L ammonium acetate in deionized water (mobile phase A) and HPLC-grade methanol (mobile phase B). Standard heated electrospray ionization (HESI) source settings were applied. The mass spectrometer operated in negative ion mode with targeted MS/MS triggered by the precursor ion at m/z 297.9573. The RF lens was set at 35 %. Full scan resolution using the orbitrap was set at 240,000 and the MS1 mass range was set to (275 to 375) *m/z*. Full scan ion target value was 4.0×10^5 allowing a maximum injection time of 50 ms. Targeted mass fragmentation was performed using higher-energy collisional dissociation (HCD) at a collision energy of 30 with quadrupole isolation at *m/z* 0.4 width. The fragment scan resolution using the orbitrap was set at 30,000, ion target value of 5.0×10^5 and 54 ms maximum injection time. Secondary targeted mass fragmentation was also performed using collisional induced

dissociation (CID) at a normalized collision energy of 35 with quadrupole isolation at *m/z* 0.4 width. The fragment scan resolution using the orbitrap was set at 30,000, ion target value of 5.0 x 10^5 and 54 ms maximum injection time.

HRMS analysis of SRM 1947a extracts did not confirm the presence of FBSA. As a result, the mass fraction reported in this ROA should not be used for certification. Future HRMS studies may be warranted to identify the structure of the interfering compound.

5.1.6. Quantitation and Results

Levels of 30 PFAS in the RMs were calculated using the linear equation of the calibration curve, not forcing the intercept through zero. Compounds were quantified using a relative response ratio to the internal standard compound that most closely matched the compound (Table 23). The reporting limits (RLs) were determined as the maximum value of either the average mass measured in the autosampler vial extract plus three times the standard deviation of the compound measured in the blanks or the lowest calibrant detected, all divided by the mass of the sample.

R^2 values greater than 0.99 were observed for all PFAS calibration curves. PFOS values measured in the control material, SRM 1947, were within the values reported on the COA [(5.76 ± 0.072) ng/g compared to (5.90 ± 0.39) ng/g]. The mass fractions reported in Table 24 are totals, including branched and linear isomers. PFOS was measured at the highest concentration (13.5 ng/g average) in SRM 1947a, and longer chain carboxylic acids were also detected in SRM 1947a.

Table 24. Mass fraction (ng/g, as received) of PFAS in SRM 1947a.

Analyte	Rep 1	Rep 2	Rep 3	Rep 4	Rep 5	Rep 6	Rep 7	Rep 8	Rep 9	Rep 10	n	Mean	SD
PFBA	<3.65	<6.89	<5.80	<3.70	<4.09	<4.93	<5.16	<4.76	<4.02	<6.55			
PFPeA	<1.20	<2.27	<1.91	<1.22	<1.35	<1.63	<1.70	<1.57	<1.32	<2.16			
PFHxA	<0.576	<1.086	<0.915	<0.584	<0.646	<0.778	<0.813	<0.751	<0.633	<1.032			
PFHpA	<0.397	<0.749	<0.631	<0.403	<0.445	<0.537	<0.561	<0.518	<0.437	<0.712			
PFOA	<0.583	<1.099	<0.926	<0.591	<0.653	<0.788	<0.823	<0.760	<0.641	<1.045			
PFNA	0.13	<0.203	<0.171	<0.109	0.16	<0.145	0.16	0.14	0.13	<0.193	5	0.146	0.016
PFDA	0.36	<0.345	0.37	0.35	0.44	0.35	0.33	0.39	0.48	0.52	9	0.398	0.064
PFUnA	0.28	0.23	0.33	0.37	0.31	0.29	0.28	0.35	0.27	0.32	10	0.302	0.041
PFDoA	<0.107	<0.203	<0.171	0.15	<0.120	<0.145	<0.152	<0.140	<0.118	<0.193	1	0.145	
PFTriA	0.34	0.23	0.20	0.20	0.20	0.20	0.18	0.16	0.21	<0.193	9	0.212	0.052
PFTA	<0.108	<0.204	<0.172	<0.110	<0.121	<0.146	<0.153	<0.141	<0.119	<0.194			
FBSA*	0.65	0.73	0.70	0.66	0.66	0.67	0.64	0.66	0.61	0.70	10	0.669	0.034
PFHxSA	<0.934	<1.760	<1.483	<0.947	<1.046	<1.261	<1.319	<1.217	<1.027	<1.673			
PFOSA	<0.107	<0.203	<0.171	<0.109	<0.120	<0.145	<0.152	<0.140	<0.118	<0.193			
HFPO-DA	<0.934	<1.760	<1.483	<0.947	<1.046	<1.261	<1.319	<1.217	<1.027	<1.673			
NMeFOSAA	<0.934	<1.760	<1.483	<0.947	<1.046	<1.261	<1.319	<1.217	<1.027	<1.673			
NEtFOSAA	<0.934	<1.760	<1.483	<0.947	<1.046	<1.261	<1.319	<1.217	<1.027	<1.673			
PFBS	<0.165	<0.312	<0.263	<0.167	<0.185	<0.223	<0.233	<0.215	<0.182	<0.296			
PFPeS	<0.107	<0.203	<0.171	<0.109	<0.120	<0.145	<0.152	<0.140	<0.118	<0.193			
PFHxS	<0.107	<0.203	<0.171	<0.109	<0.120	<0.145	<0.152	<0.140	<0.118	<0.193			
PFHpS	<0.171	<0.322	<0.272	<0.173	<0.191	<0.231	<0.241	<0.223	<0.188	<0.306			
PFOS	12.80	13.30	13.90	12.70	14.40	14.30	13.30	13.40	13.50	13.60	10	13.52	0.56
PFNS	<0.107	<0.203	<0.171	<0.109	<0.120	<0.145	<0.152	<0.140	<0.118	<0.193			
PFDS	<0.189	<0.357	<0.301	<0.192	<0.212	<0.256	<0.267	<0.247	<0.208	<0.339			
4:2FTS	<0.107	<0.203	<0.171	<0.109	<0.120	<0.145	<0.152	<0.140	<0.118	<0.193			
6:2FTS	<0.107	<0.203	<0.171	<0.109	<0.120	<0.145	<0.152	<0.140	<0.118	<0.193			
8:2FTS	<0.179	<0.337	<0.284	<0.181	<0.200	<0.242	<0.253	<0.233	<0.197	<0.321			
NaDONA	<0.107	<0.203	<0.171	<0.109	<0.120	<0.145	<0.152	<0.140	<0.118	<0.193			

*Unconfirmed measurements not used in value assignment.

The homogeneity of SRM 1947a was assessed by plotting the PFAS mass fractions versus jar packaging order as shown in Fig. 20.

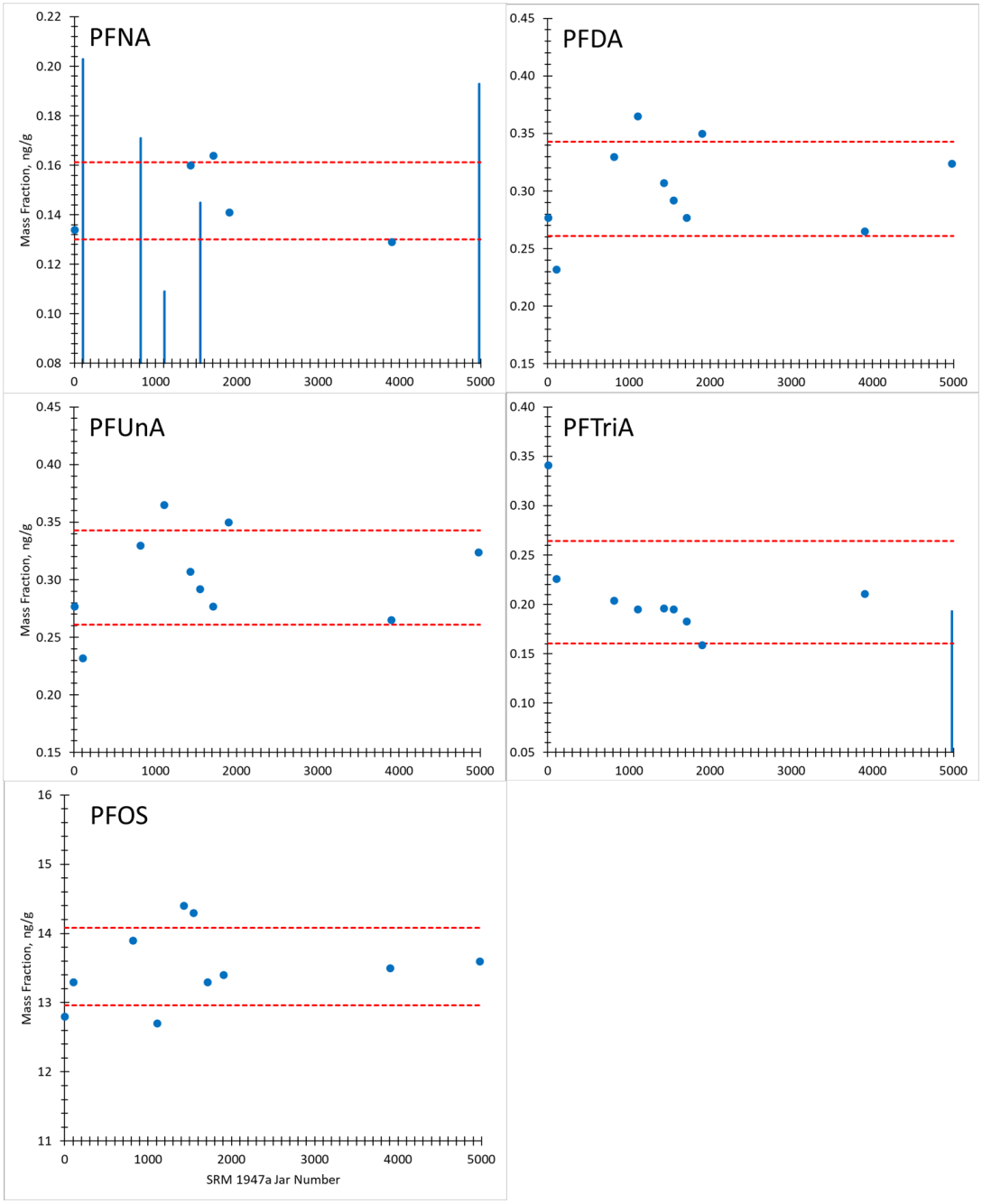

Fig. 20. Homogeneity Assessment for SRM 1947a as a Function of Sample Jar Number.

Solid circles represent PFAS mass fractions results (ng/g) that meet measurement quality criteria; vertical lines represent results that were determined only as upper-bound values. The results are plotted as functions of jar packaging sequence. Dashed horizontal lines bound intervals defined as (mean ± standard deviation) of the fully quantitative results.

5.2. PFAS Analysis Method 2

5.2.1. Materials

All solvents were obtained from Thermo Fisher (Optima LC-MS; Waltham, MA). Target PFAS were analyzed using NIST reference materials (RM) 8446 Perfluorinated Carboxylic Acids and Perfluorooctane Sulfonamide in Methanol and RM 8447 Perfluorinated Sulfonic Acids in Methanol. An isotopically labeled PFAS mixture (MPFAC-24ES, 1000 ng/mL in methanol, Wellington Laboratories, Guelph, Ontario, Canada) used for internal standard. SRM 1946 was used as a quality control material. All glassware and lab supplies were rinsed with methanol prior to use. Original QuEChERS extractions salt ECMSSCFS-MP with 6000 mg $MgSO_4$ and 1500 mg NaCl and QuEChERS dSPE ECMPSCB-MP with 900 mg $MgSO_4$, 300 mg PSA, and 150 mg graphitized carbon black were purchased from United Chemical Technologies (UCT, Bristol, PA).

5.2.2. Calibration Preparation

RMs 8446 and 8447 were combined in methanol-rinsed glassware and gravimetrically diluted with methanol to create three working stock solutions which were then gravimetrically diluted to produce eight calibration working solutions. The calibration solutions contained 15 PFAS (Table 25) in a range from approximately 0.05 ng/g to 30 ng/g. The internal standard solution contained 15 isotopically labeled PFAS (Table 26) present at approximately 5.3 ng/g.

Table 25. Composition of PFAS Calibration Stock Solution.

Analyte	Abbreviation	Source Material	Mass Fraction, µg/g
Perfluorobutane sulfonate	PFBS	RM 8447	42.3
Perfluorohexane sulfonate	PFHxS	RM 8447	55.2
Perfluorooctane sulfonate	PFOS	RM 8447	56.6
Perfluorohexanoic acid	PFHxA	RM 8446a	59.1
Perfluoroheptanoic acid	PFHpA	RM 8446a	76.0
Perfluorooctanoate acid	PFOA	RM 8446a	54.8
Perfluorononanoic acid	PFNA	RM 8446a	63.0
Perfluorodecanoic acid	PFDA	RM 8446a	58.1
Perfluoroundecanoic acid	PFUnA	RM 8446a	62.8
Perfluorododecanoic acid	PFDoA	RM 8446a	59.5
Perfluorotridecanoic acid	PFTriA	RM 8446a	62.9
Perfluorotetradecanoic acid	PFTA	RM 8446a	58.0
Perfluorobutanoic acid	PFBA	RM 8446b	43.0
Perfluoropentanoic acid	PFPeA	RM 8446b	60.9
Perfluorooctane sulfonamide	PFOSA	RM 8446b	66.9

Table 26. Composition of PFAS Internal Standard Stock Solution.

PFAS	Internal Standard	Abbreviation	Mass Concentration ng/mL
PFBS	Sodium perfluoro-1-(2,3,4-$^{13}C_3$)butanesulfate	IS-PFBS	932
PFHxS	Sodium perfluoro-1-(1,2,3-$^{13}C_3$)hexanesulfate	IS-PFHxS	948
PFOS	Sodium perfluoro-1-($^{13}C_8$)hexanesulfate	IS-PFOS	959
PFHxA	Perfluoro-n-(1,2,3,4,6-$^{13}C_5$)hexanoic acid	IS-PFHxA	1000
PFHpA	Perfluoro-n-(1,2,3,4-$^{13}C_4$)heptanoic acid	IS-PFHpA	1000
PFOA	Perfluoro-n-($^{13}C_8$)octanoic acid	IS-PFOA	1000
PFNA	Perfluoro-n-($^{13}C_9$)nonanoic acid	IS-PFNA	1000
PFDA	Perfluoro-n-(1,2,3,4,5,6-$^{13}C_6$)decanoic acid	IS-PFDA	1000
PFUnA	Perfluoro-n-(1,2,3,4,5,6,7-$^{13}C_7$)undecanoic acid	IS-PFUnA	1000
PFDoA	Perfluoro-n-(1,2-$^{13}C_2$)dodecanoic acid	IS-PFDoA	1000
PFTriA	Perfluoro-n-(1,2-$^{13}C_2$)dodecanoic acid	IS-PFDoA	1000
PFTA	Perfluoro-n-(1,2-$^{13}C_2$)tetradecanoic acid	IS-PFTA	1000
PFBA	Perfluoro-n-($^{13}C_4$)butanoic acid	IS-PFBA	1000
PFPeA	Perfluoro-n-($^{13}C_5$)pentanoic acid	IS-PFPeA	1000
PFOSA	Perfluoro-1-($^{13}C_8$)octanesulfonamide	IS-PFOSA	1000

5.2.3. Sample Preparation

Eight calibrants, three blanks (DI water), three replicates from the same jar of SRM 1946, and six replicates from the same jar of SRM 1947a were prepared. Extraction and cleanup were carried out using a modified QuEChERS method [24]. First, approximately 1 g of sample and 200 µL of internal standard working solution were gravimetrically weighed into a 50-mL PP centrifuge tube. Then 10 mL of acetonitrile and 150 µL of formic acid were added to the tube and vortexed for 1 min. The first QuEChERS salt packet (extraction salt ECMSSCFS-MP) was then added to the tube, vortexed, sonicated for 10 min, then vortexed for 5 min at 753 RCF (2500 rpm). The supernatant was transferred to a 15-mL centrifuge tube already containing the dSPE sorbent (ECMPSCB-MP). The 15-mL PP centrifuge tube was vortexed for 2 min and then centrifuged for 5 min at 753 RCF (2500 rpm). The resulting supernatant was filtered with an 0.2 µm syringe filter into a new 15-mL centrifuge tube and dried under nitrogen to a final volume of approximately 1 mL, and then transferred a precleaned autosampler vial for analysis via LC-MS/MS.

5.2.4. Instrumental method

A similar LC-MS/MS analysis was performed, using an Agilent Infinity II (Agilent, Santa Clara, CA) connected to an AB Sciex API 5500 Triple Quadrupole Mass Spectrometer (AB Sciex, Framingham, MA). The autosampler tray temperature was set to the ambient air temperature, roughly 25 °C. Chromatographic separation was achieved using a Zorbax Diol (4.6 mm i.d., 12.5 mm, 6 µm particle size) guard column attached to an Agilent InfinityLab Poroshell 120 EC-C18 column (4.6 mm i.d., 100 mm, 2.7 µm particle size) column, maintained at ambient air temperature for the entire run. The mobile phases consisted of 10 mmol/L ammonium acetate in 90 % laboratory deionized water and 10 % methanol (A) and 10 mmol/L ammonium acetate in methanol (B) with a flow rate of 0.3 mL/min and initial composition of 100 % A, 0 % B. The

mobile phase gradient program was as follows: 100 % A, 65 % A at 3 min, 0 % A at 25 min, held at 0 % A for 7 min, 100 % A at 32.2 min and held at 100 % A until 45 min. A retention column was placed before the pumps (Eclipse Plus C18, 4.6 mm i.d., 50 mm, 5 µm particle size) to separate instrumental contamination. Mass spectrometric detection was performed in electrospray ionization (ESI) in negative (-) mode, using a scheduled multiple reaction monitoring method (MRM). Source parameters were the same as those used in method 1. Compound specific parameters are listed in Table 27.

Table 27. Analyte-Specific LC-MS/MS Parameters.

Analyte	Q1[a] *m/z*	Q3[b] *m/z*	RT[c] min	DP[d] volts	CE[e] volts	Analyte	Q1[a] *m/z*	Q3[b] *m/z*	RT[c] min	DP volts	CE volts
IS-PFBA	217	172	13.9	-70	-20	IS-PFOS	507	99	25.7	-60	-60
PFBA	213	169	13.9	-70	-20	PFNA 1	463	419	25.8	-70	-20
PFPeA 1	263	219	17.9	-70	-20	PFNA 2	469	219	25.8	-70	-30
IS-PFPeA	268	223	17.9	-70	-20	IS-PFNA	472	427	25.8	-70	-20
PFBS 1	299	80	18.4	-70	-70	PFDA 1	513	469	26.9	-80	-20
PFBS 2	299	99	18.4	-70	-70	PFDA 2	513	219	26.9	-70	-30
IS-PFBS	302	99	18.4	-70	-70	IS-PFDA	519	474	26.9	-80	-20
PFHxA 1	313	269	20.7	-70	-10	PFOSA 1	498	78	27.6	-70	-70
PFHxA 2	313	119	20.7	-50	-10	PFOSA 2	498	169	27.6	-70	-40
IS-PFHxA	318	273	20.7	-70	-10	IS-PFOSA	506	78	27.6	-70	-70
PFHxS 1	399	80	22.3	-60	-60	PFUnA 1	563	519	27.9	-70	-20
PFHxS 2	399	99	22.3	-60	-60	PFUnA 2	563	269	27.9	-70	-20
IS-PFHxS	402	99	22.3	-60	-60	IS-PFUnA	570	525	27.9	-70	-20
PFHpA 1	363	319	22.7	-70	-20	PFDoA 1	613	569	28.7	-70	-20
PFHpA 2	363	169	22.7	-70	-20	PFDoA 2	613	269	28.7	-70	-60
IS-PFHpA	367	322	22.7	-70	-20	IS-PFDoA	615	570	28.7	-70	-20
PFOA 1	413	369	24.4	-70	-20	PFTriA 1	663	619	29.4	-70	-20
PFOA 2	413	169	24.4	-70	-30	PFTriA 2	663	269	29.4	-70	-70
IS-PFOA	421	376	24.4	-70	-20	PFTA 1	713	669	30	-70	-20
PFOS 1	499	80	25.7	-60	-60	PFTA 2	713	369	30	-70	-50
PFOS 2	499	99	25.7	-60	-60	IS-PFTA	715	670	30	-70	-20

a Mass/charge ratio of precursor ion
b Mass/charge ratio of product ion
c Peak retention time
d Declustering potential
e Collision energy

5.2.5. Quantitation and Results

Peak integration was performed in SCIEX Analyst 1.6.3. PFAS identification in samples was confirmed by retention time matching with calibration solutions. PFAS calibration slopes and intercepts were determined with linear regressions of instrument response (e.g., peak area) ratio of unlabeled analyte to labeled internal standard against the mass ratio of unlabeled analyte to labeled internal standard. Calibration regressions were only considered if at least five consecutive calibration standards (R^2) value of >0.995 in the linear range. LODs were determined by the lowest calibration point, or average mass fraction measured in the blanks plus three times the standard deviation of the blanks, whichever was highest.

Direct comparisons were only made for compounds that had detections above the LOD in both the current analyses and previous measurements, either provided on a COA or in an ROA. Some compounds had elevated LODs due to transition detections in blanks. These include PFPeA (1.42 ng/g to 2.11 ng/g), PFHxA (6.22 ng/g to 8.47 ng/g), PFHpA (37.39 ng/g to 55.71 ng/g), and PFOA (1.81 ng/g to 2.69 ng/g).

Mass fractions (ng/g) of PFAS in the individual preparations of SRM 1946, mean, 1 standard deviation, and comparison to the COA values are listed in Table 28. The mass fractions of PFAS in the individual preparations of SRM 1947a, mean, and 1 standard deviation are listed in

a The number of replicates with values above background.
b The mean of the replicates with values above background.
c The standard deviation of the replicates with values above background.

Table 29.

Table 28: PFAS Method 2 Mass Fractions (ng/g) in SRM 1946

Analyte	n_r[a]	Mean[b]	SD[c]	COA Value[b]	U_{95}
PFBA	3	1.52	0.50	-	-
PFNA	3	0.146	0.031	-	-
PFDA	3	0.151	0.026	-	-
PFOSA	3	0.181	0.010	-	-
PFUnA	3	0.401	0.006	-	-
PFOS	3	1.873	0.057	2.19	0.08

a The number of replicates with values above background.
b The mean of the replicates with values above background.
c The standard deviation of the replicates with values above background.

Table 29: PFAS Method 2 Mass Fraction (ng/g) in SRM 1947a

Analyte	Rep 1	Rep 2	Rep 3	Rep 4	Rep 5	Rep 6	n_r[a]	Mean[b]	SD[c]
PFBA	1.59	1.27	0.87	1.01	1.37	1.37	6	1.25	0.26
PFHxS	0.120	0.100	0.109	0.112	0.120	0.113	6	0.304	0.050
PFNA	0.218	0.273	0.348	0.331	0.340	0.311	6	0.336	0.019
PFDA	0.325	0.325	0.360	0.310	0.352	0.342	6	0.303	0.009
PFOSA	0.200	0.183	0.171	0.176	0.188	0.178	6	0.183	0.010
PFUnA	<0.349	0.301	0.318	0.294	0.300	0.300	5	0.112	0.008
PFOS	11.1	10.6	10.7	10.9	10.9	10.7	6	10.82	0.18

a The number of replicates with values above background.
b The mean of the replicates with values above background.
c The standard deviation of the replicates with values above background.

5.3. PFAS Analysis Method 3

SRM 1947a was used as the control material in a study observing PFAS levels in muscle tissue and liver tissue of aquaculturally-raised juvenile red drum (Sciaenops ocellatus). Only the results of SRM 1947a are discussed here.

5.3.1. Materials

All solvents were obtained from Thermo Fisher (Optima LC-MS; Waltham, MA). Target PFAS were measured using a native PFAS standard stock solution in methanol (1000 ng/mL) and an isotopically labeled PFAS mixture (MPFAC-24ES, 1000 ng/mL in methanol) both obtained from Wellington Laboratories (Guelph, Ontario, Canada).

5.3.2. Calibration Preparation

The PFAS standard stock solution contained 30 PFAS (Table 23). The stock solution was gravimetrically diluted in methanol to prepare eight calibration solutions, ranging from 0.52 ng/g to 79.9 ng/g. The IS stock solution contained 19 isotopically ^{13}C-labeled PFAS (Table 23) and was gravimetrically diluted to obtain a final concentration of approximately 2.2 ng/g.

5.3.3. Sample Preparation

Samples were prepared in similarly to that described in Section 5.1.3. The only difference was the 6 mL of methanol was used to rinse the ENVI-Carb cartridge and 6 mL of methanol was used to elute the target analytes from the cartridge. The first set of test samples were prepared alongside eight calibrants, three blanks (DI water), and eight replicates (from one jar) of SRM 1947a and second set of test samples were prepared along with eight calibrants, three blanks (DI water), and four replicates (from one jar) of SRM 1947a.

5.3.4. Instrumental method

The LC-MS/MS analysis was identical to that described in Section 5.1.4 with one exception. performed. The mobile phases consisted of 10 mmol/L ammonium acetate in 90 % laboratory nanopure water and 10 % methanol (A) and 10 mmol/L ammonium acetate in methanol (B).

5.3.5. Quantitation and Results

Levels of 30 PFAS in the samples were calculated using the Microsoft Excel based program EMMA (version 2.14) [20] which employs a linear equation of the calibration curve. Compounds were quantified using a relative response ratio to the internal standard compound that most closely matched the compound. The RL was determined as the mean concentration of the blanks plus three times the standard deviation of that concentration in the blanks. R^2 values of ≥ 0.99 were observed for all PFAS calibration curves. Of the 30 PFAS measured in the tissue and

liver test samples, PFOS was the only compound detected above the RL. Table 30 shows the PFOS measured in SRM 1947a from both analyses.

Table 30: PFAS Method 3 Mass Fractions (ng/g) in SRM 1947a

	Sample Set 1			Sample Set 2			Combined		
Analyte	n_r[a]	Mean[b]	SD[c]	n_r[a]	Mean[b]	SD[c]	n_c[d]	Value[e]	SD[f]
PFOS	8	15.20	0.52	4	11.7	2.2	2	13.5	2.5

a The number of replicates with values above background.
b The mean of the replicates with values above background.
c The standard deviation of the replicates with values above background.
d The number of calibrations yielding one or more results above background.
e When both calibrations yielded a result above background, the mean of the two means.
When only one calibration yielded a result above background, the mean of that calibration.
f The standard deviation of the calibration means.

5.4. Comparison of PFAS Results

Combination of the PFAS method results are listed in Table 31.

Table 31: Combined Results for PFAS in SRM 1947a, ng/g.

Analyte	n_m[a]	Value[b]	SD[c]
PFBA	1	1.25	
PFNA	2	0.22	0.11
PFDA	2	0.37	0.04
PFUnA	2	0.3023	0.0005
PFDoA	1	0.15	
PFTriA	1	0.21	
FBSA*	1	0.67	
PFOSA	1	0.18	
PFHxS	1	0.11	
PFOS	4	12.8	2.0

a The number of Methods yielding one or more results above background.
b When both Methods yielded a result above background, the mean of the two summary values.
When only one Method yielded a result above background, the summary value of that Method.
c The standard deviation of the Method values.
*Unconfirmed measurements not to be used in value assignment.

5.4.1. Metrological Traceability

The PFAS values are comprised of both linear and branched isomers (totals), and the results are metrologically traceable to the commercial analytical standards used as calibrants. The PFAS results are not traceable to the SI.

6. Value Assignment Calculations

Statistical analysis was provided by the NIST Statistical Engineering Division.

6.1. Analyte Evaluated Using a Single Method

The value and uncertainties for an analyte, *y*, evaluated using just one measurement method are calculated using the following model:

$$y_i = \mu + \varepsilon_i,\ i = 1, 2, \ldots, n \quad (7)$$

where *i* indexes replication, μ is the true value, *n* represents the number of replications, and $\varepsilon_i \sim N(0, \sigma^2)$ – which is compact notation for "the measured differences from the mean value are independent and identically distributed random variates from a normal (Gaussian) distribution of mean zero and standard deviation σ". The assigned value is the arithmetic mean of the y_i, $\bar{y}$, which is an estimate of μ. The standard uncertainty of the mean, $u(\bar{y})$, is the standard deviation of the y_i divided by the square root of the number of replications. The approximately 95 % coverage expanded uncertainty, $U_{95}(\bar{y})$, is estimated using the Student's *t* 0.975 confidence level for *n*-1 degrees of freedom, $t_{0.975,n-1}$, as the coverage factor:

$$U_{95}(\bar{y}) = t_{0.975,n-1} \times u(\bar{y})\ . \quad (8)$$

6.2. Analyte Evaluated Using Multiple Methods

The value and uncertainties for an analyte, *y*, evaluated using two or more measurement methods are calculated using the following model:

$$y_{ij} = \mu + m_i + \varepsilon_{ij};\ i = 1, 2, \ldots, n_{mm};\ j = 1, 2, \ldots, n_i \quad (9)$$

where *i* indexes measurement methods, *j* indexes replication within measurement method, n_{mm} represents the number of measurement methods, n_i represents the number of replications within measurement method, and m_i and ε_{ij} are independent and identically $N(0, \sigma^2)$-distributed (iid) random variables that are independent of method. The assigned value is the DerSimonian-Laird consensus estimator of μ, $\bar{y}_{DL}$ [25]. The standard, $u(\bar{y}_{DL})$, and 95 % coverage expanded, $U_{95}(\bar{y}_{DL})$, uncertainties were determined using the Horn-Horn-Duncan (HHD) method for variances [26].

7. Certificate of Analysis

The results of the statistical analysis for all analytes are presented in the Certificate of Analysis (COA) for SRM 1947a Great Lakes Fish Tissue. A NIST COA is defined below.

"In accordance with ISO Guide 31: 2000, a NIST SRM certificate is a document containing the name, description, and intended purpose of the material, the logo of the U.S. Department of Commerce, the name of NIST as a certifying body, instructions for proper use and storage of the material, certified property value(s) with associated uncertainty(ies), method(s) used to obtain property values, the period of validity, if appropriate, and any other technical information deemed necessary for its proper use. A Certificate is issued for an SRM certified for one or more specific physical or engineering performance properties and may contain NIST reference, information, or both values in addition to certified values. A Certificate of Analysis is issued for an SRM certified for one or more specific chemical properties. Note: ISO Guide 31 is updated periodically; check with ISO for the latest version." [27]

For the most current version of the COA for NIST SRM 1947a, please visit: https://www-s.nist.gov/srmors/view_detail.cfm?srm=1947a.

References

[1] National Institute of Standards and Technology (2-September-2020) Certificate of Analysis, Standard Reference Material 1946 Lake Superior Fish Tissue. https://tsapps.nist.gov/srmext/certificates/archives/1946.pdf.

[2] National Institute of Standards and Technology (3-September-2020) Certificate of Analysis, Standard Reference Material 1947 Lake Michigan Fish Tissue. https://tsapps.nist.gov/srmext/certificates/1947.pdf.

[3] Ellisor, D. , Moors, A. , Hoguet, J. , Ness, J. , Capuano, A. and Franco, O. (2024), Homogenization of Large Batch Frozen Materials Using the Palla-VM-KT Vibrating Mill, Special Publication (NIST SP), National Institute of Standards and Technology, Gaithersburg, MD, https://doi.org/10.6028/NIST.SP.1196r1 , https://tsapps.nist.gov/publication/get_pdf.cfm?pub_id=957773 (Accessed September 17, 2025).

[4] ISO (2020) ISO Standard 13320:2020 Particle size analysis — Laser diffraction methods. International Organization for Standardization (ISO). Geneva. https://www.iso.org/standard/69111.html.

[5] U.S. EPA (1998) Method 7473 (SW-846): Mercury in Solids and Solutions by Thermal Decomposition, Amalgamation, and Atomic Absorption Spectrophotometry," Revision 0. https://www.epa.gov/esam/epa-method-7473-sw-846-mercury-solids-and-solutions-thermal-decomposition-amalgamation-and. Accessed 9/17/2025.

[6] Milestone (2019) Industry Report: Determination of Total Mercury in Environmental Samples. https://www.milestonesci.com/wp-content/uploads/2019/07/Industry-report-DMA-80-Environmental-USREV062019.pdf. Accessed 9/17/2025.

[7] National Institute of Standards and Technology (2-July-2025) Certificate of Analysis, Standard Reference Material 3133 Mercury Standard Solution Lot No. 160921. https://tsapps.nist.gov/srmext/certificates/3133.pdf.

[8] Christopher SJ, Long SE, Rearick MS, Fassett JD (2001) Development of High Accuracy Vapor Generation Inductively Coupled Plasma Mass Spectrometry and its Application to the Certification of Mercury in Standard Reference Materials. Anal Chem 73(10):2190-2199. https://doi.org/10.1021/ac0013002.

[9] Ragland JM, Long SE (2022) Data Tool Development Series: Isotope Dilution Assistant (IDA) v1.0. https://github.com/jmr-nist-gov/IDA.

[10] Possolo A, van der Veen AMH, Meija J, Hibbert DB (2018) Interpreting and propagating the uncertainty of the standard atomic weights (IUPAC Technical Report). Pure Appl Chem 90:395-424. https://doi.org/10.1515/pac-2016-0402.

[11] IUPAC Commission on Isotopic Abundances and Atomic Weights (CIAAW), molecular weight calculator. https://ciaaw.shinyapps.io/calculator/. Accessed 9/17/2025.

[12] Meija J, Coplen TB, Berglund M, Brand WA, De Bièvre P, Gröning M, Holden NE, Irrgeher J, Loss RD, Walczyk T, Prohaska T (2016) Isotopic compositions of the elements 2013 Pure and Applied Chemistry 88, 293-306. https://doi.org/10.1515/pac-2015-0503. See also: IUPAC Commission on Isotopic Abundances and Atomic Weights (CIAAW). Isotopic compositions of the elements 2021. Available online at www.ciaaw.org.

[13] The United Nations Environment Programme (UNEP) (2024) Why do persistent organic pollutants matter? https://www.unep.org/topics/chemicals-and-pollution-action/pollution-and-health/persistent-organic-pollutants-pops/why Accessed 9/22/2025.
[14] U.S. Environmental Protection Agency (2002, Updated 2009 and 2025) Persistent Organic Pollutants: A Global Issue, A Global Response https://www.epa.gov/international-cooperation/persistent-organic-pollutants-global-issue-global-response Accessed 9/22/2025.
[15] National Institute of Standards and Technology (14-August-2018) Certificate of Analysis, Standard Reference Material 2257 PBDE Congeners in 2,2,4-Trimethylpentane. https://tsapps.nist.gov/srmext/certificates/2257.pdf.
[16] National Institute of Standards and Technology (11-September-2018) Certificate of Analysis, Standard Reference Material 2258 BDE 209 in 2,2,4-Trimethylpentane. https://tsapps.nist.gov/srmext/certificates/2258.pdf.
[17] National Institute of Standards and Technology (17-May-2017) Certificate of Analysis, Standard Reference Material 2259 Polychlorinated Biphenyl Congeners in 2,2,4-Trimethylpentane. https://tsapps.nist.gov/srmext/certificates/2259.pdf.
[18] National Institute of Standards and Technology (28-Jun-2018) Certificate of Analysis, Standard Reference Material 2261 Chlorinated Pesticides in Hexane. https://tsapps.nist.gov/srmext/certificates/2261.pdf.
[19] National Institute of Standards and Technology (22-April-2020) Certificate of Analysis, Standard Reference Material 2275 Chlorinated Pesticide Solution-II in 2,2,4-Trimethylpentane. https://tsapps.nist.gov/srmext/certificates/2275.pdf.
[20] National Institute of Standards and Technology (2014) Environmental Metrology Measurement Assistant (EMMA), Version 1. https://www.nist.gov/programs-projects/environmental-metrology-measurement-assistant-emma. Accessed 9/17/2025.
[21] Kwiatkowski CF, Andrews DQ, Birnbaum LS, Bruton T A, DeWitt JC, Knappe DRU, Maffini MV, Miller MF, Pelch KE, Reade A, Soehl A, Trier X, Venier M, Wagner CC, Wang Z, Blum A (2020) Scientific Basis for Managing PFAS as a Chemical Class. Environ Sci Technol Lett 7(8):532–543. https://doi.org/10.1021/acs.estlett.0c00255.
[22] National Institute of Standards and Technology (12-Feb-2025) Certificate of Analysis, Standard Reference Material 2585 Organic Contaminants in House Dust. https://tsapps.nist.gov/srmext/certificates/2585.pdf.
[23] National Institute of Standards and Technology (28-May-2025) Certificate of Analysis, Standard Reference Material 2781 Domestic Sludge. https://tsapps.nist.gov/srmext/certificates/2781.pdf.
[24] U.S. FDA (2024) Method C-010.03: Determination of 30 Per and Polyfluoroalkyl Substances (PFAS) in Food and Feed using Liquid Chromatography-Tandem Mass Spectrometry (LC-MS/MS) https://www.fda.gov/media/131510/download. Accessed 9/17/2025.
[25] DerSimonian R, Laird N (1986) Meta-Analysis in Clinical Trials. Control Clin Trials 7(3):177 188. https://doi.org/10.1016/0197-2456(86)90046-2.

[26] Horn SD, Horn RA, Duncan DB (1975) Estimating Heteroscedastic Variances in Linear Models. J Am Stat Assoc, 70(350):380-385. https://doi.org/10.2307/2285827.
[27] National Institute of Standards and Technology. SRM Definitions. https://www.nist.gov/srm/srm-definitions. Accessed 9/17/2025.

Appendix A. List of Acronyms

ASV	autosampler vial
CRM	certified reference material
DC-AAS	direct combustion atomic absorption spectrometry
DCM	dichloromethane
ECNI	electron capture negative chemical ionization
EI	electron impact ionization
FBSA	perfluorobutane sulfonamide
GC	gas chromatograph
GC-MS	gas chromatography mass spectrometry
HRMS	high-resolution mass spectrometry
ID-CV-ICP-MS	isotope dilution cold-vapor inductively coupled plasma mass spectrometry
IS	internal standard
IS-WS	internal standard working solution
LN_2	liquid nitrogen
LOD	limit of detection
MS	mass spectrometer
N_2	dry nitrogen gas
NIST	National Institute of Standards and Technology
PCB	polychlorinated biphenyl
PBDE	polybrominated diphenyl ether
PFE	pressurized fluid extraction
PFAA	perfluoroalkyl acid
PFAS	polyfluoroalkyl substance
PFOS	perfluorooctane sulfonic acid
POP	Persistent Organic Pollutant
PP	polypropylene
RL	reporting limit
SEC	size exclusion chromatography
SI	International System of Units
SIM	selected ion monitoring
SPE	solid phase extraction
SRM	Standard Reference Material (a NIST CRM)
TEO	Total Extractable Organics
USGS	United States Geological Survey